

THE CATHOLIC
UNIVERSITY
OF AMERICA



HELLENIC REPUBLIC
National and Kapodistrian
University of Athens



Solar wind mesoscale structures: properties and geo-effectiveness

Simone Di Matteo^{1,2}

¹ Catholic University of America, USA

² NASA – Goddard Space Flight Center, USA

13 May 2025

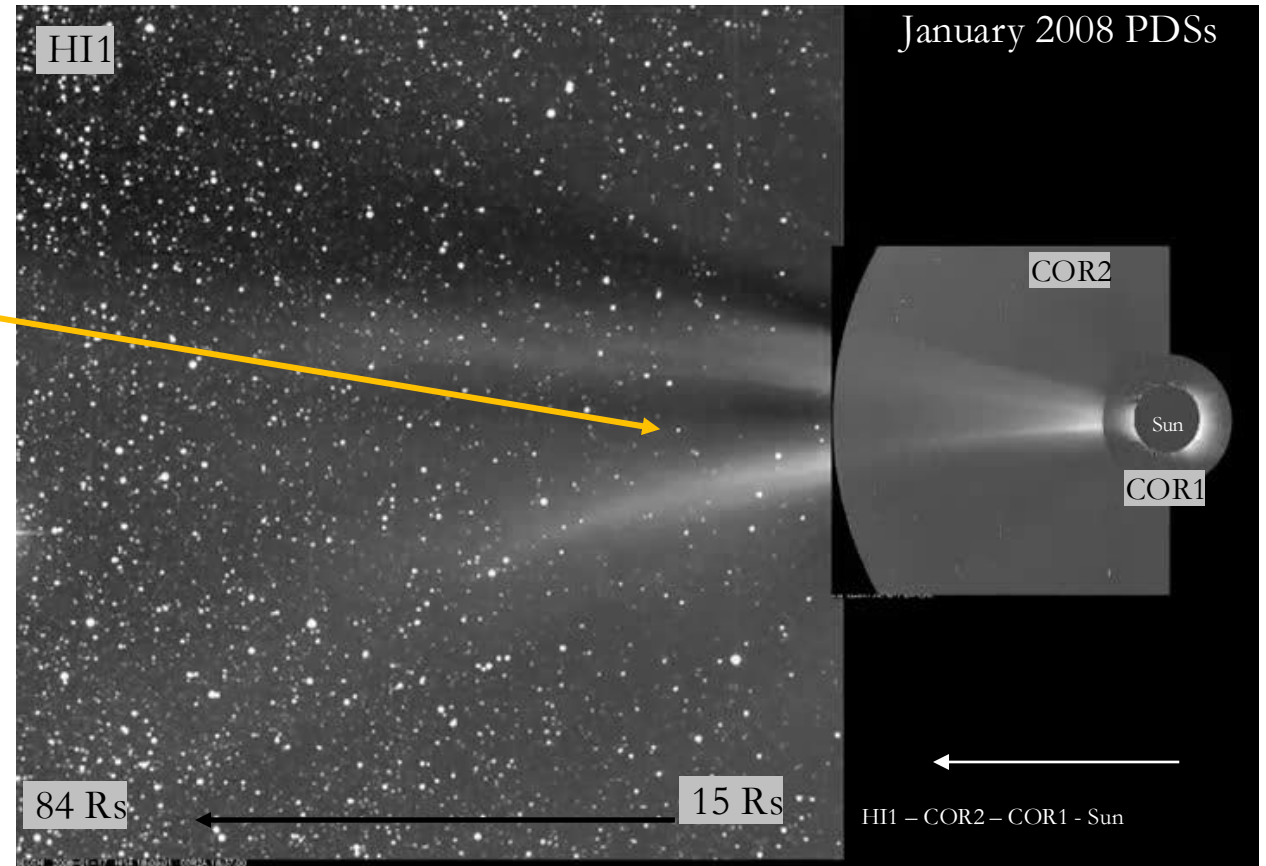
Thanks to the many collaborators: Nicki Viall, Larry Kepko, Christos Katsavrias, Umberto Villante, Nathalia Alzate and many others

Supported by NASA Grant 80NSSC21K0459

Mesoscale structures might be imposed/injected from the Sun; it is unclear what process might generate them *en route*

White light images from coronagraphs and imager on board the STEREO spacecraft show structures coming out from the Sun, sometimes in a **periodic** manner (typically ≈ 90 min).

Periodic mesoscale structures in the solar wind are typically referred to as Periodic Density Structures (PDSs)



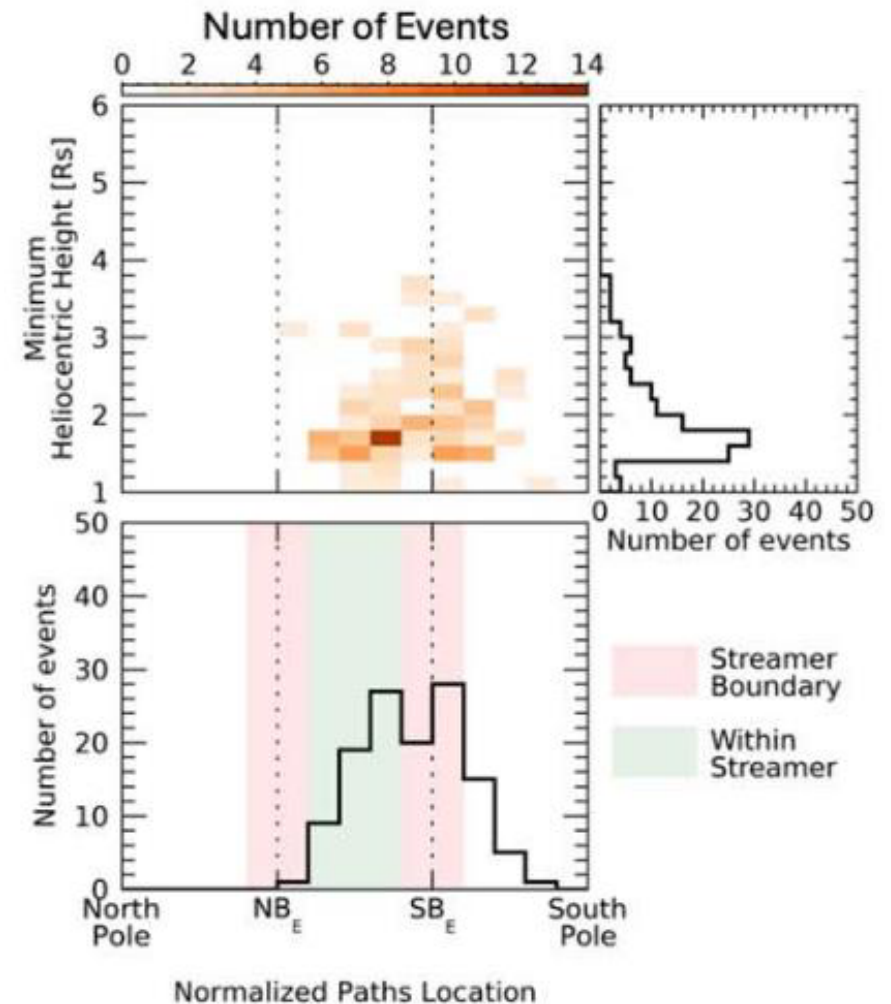
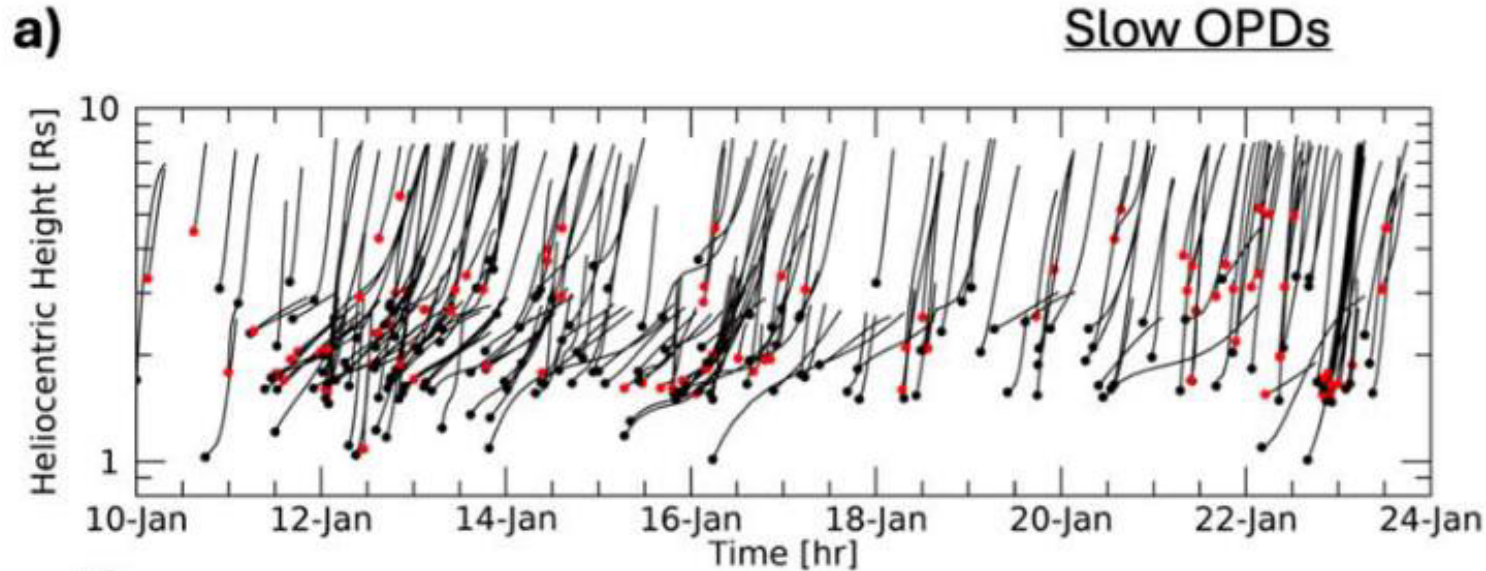
Credit: [Viall & Vourlidas 2015](#).
Courtesy of Nathalia Alzate.

Uninterrupted view of the solar corona is crucial to fully understand the origin of these mesoscale structures



Alzate, Di Matteo et al., (2024); animation available at <https://zenodo.org/records/11211569>

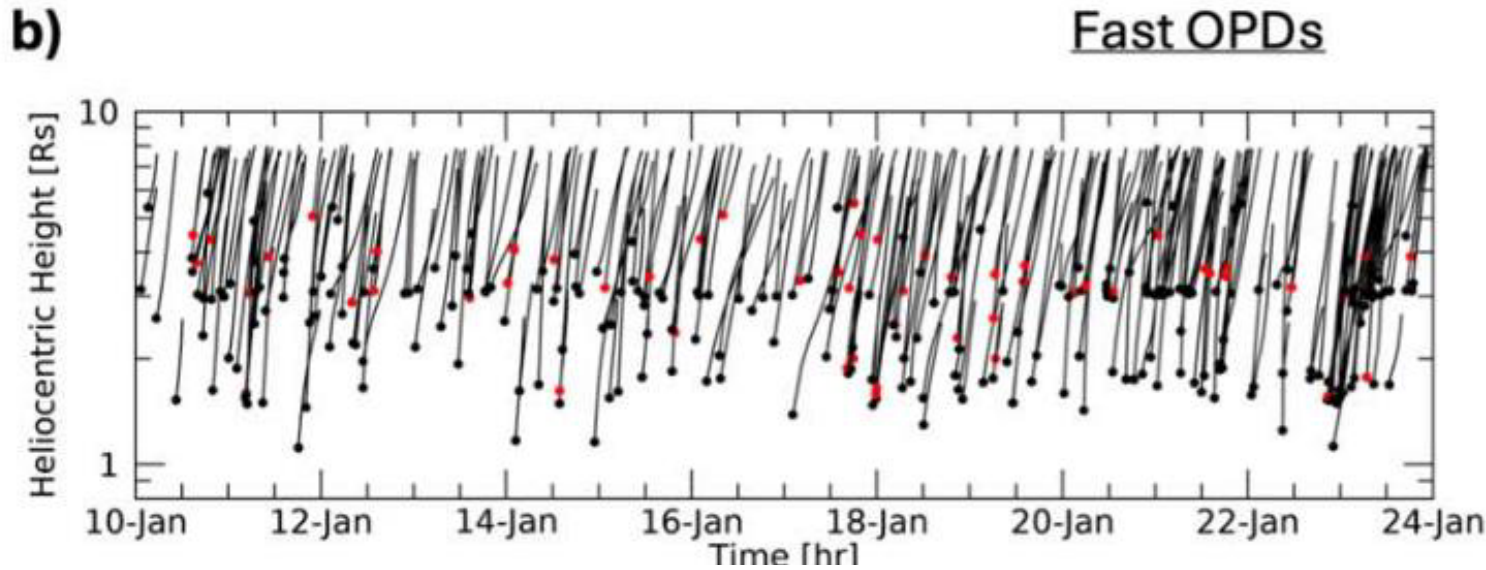
We can distinguish two classes of outward propagating disturbances (OPD): fast and slow OPDs



Slow OPDs form preferentially at ≈ 1.6 Rs closer to the streamer boundaries, with asymmetric occurrence rates

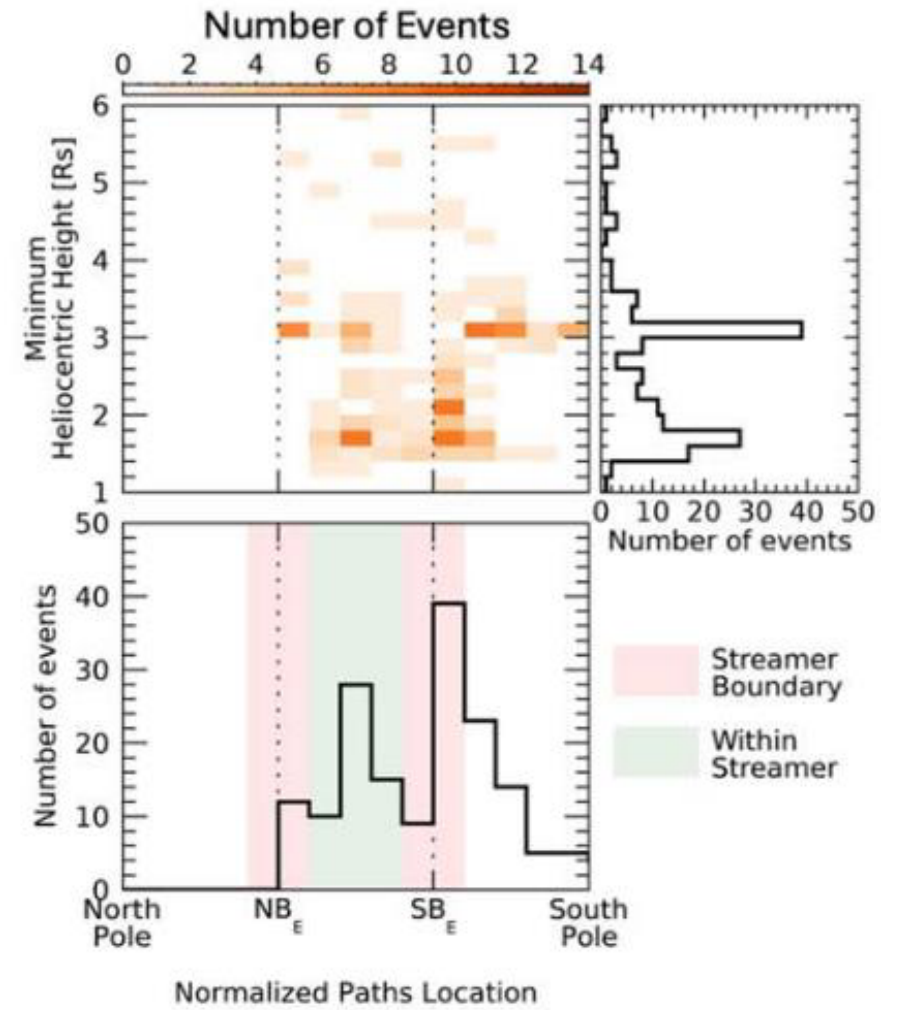
They show speeds of ≈ 16 km/s at 1.5 Rs and accelerate up to ≈ 200 km/s at 7.5 Rs.

We can distinguish two classes of outward propagating disturbances (OPD): fast and slow OPDs

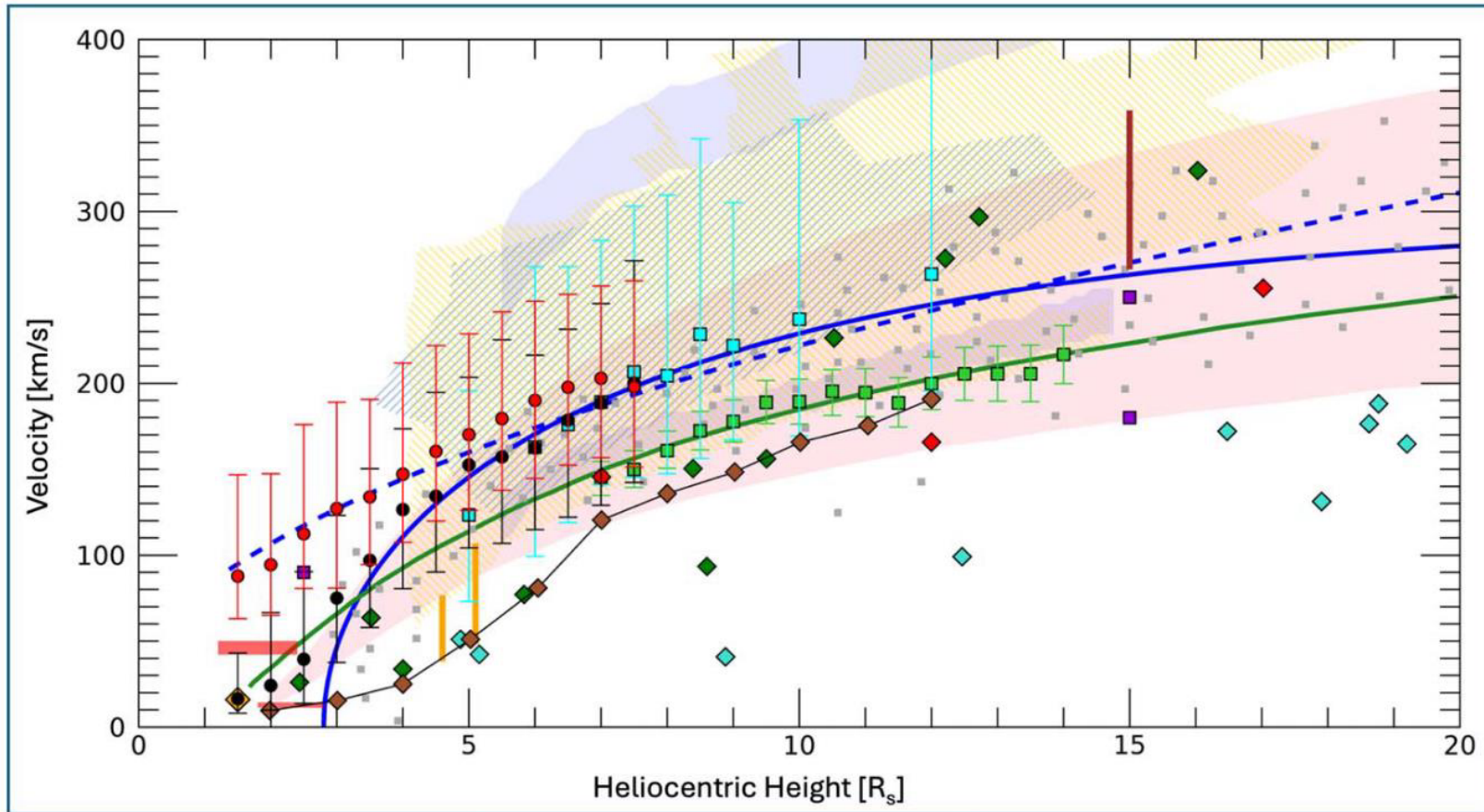


Fast OPDs form preferentially at $\approx 1.6 R_s$ and at $\approx 3.0 R_s$ both at the streamer boundaries and slightly more often within them.

They show speeds of 90 km/s at 1.5 R_s up to 200 km/s at 7.5 R_s .



Without observations below $\approx 3 R_s$, the two classes of propagating disturbances would be indistinguishable

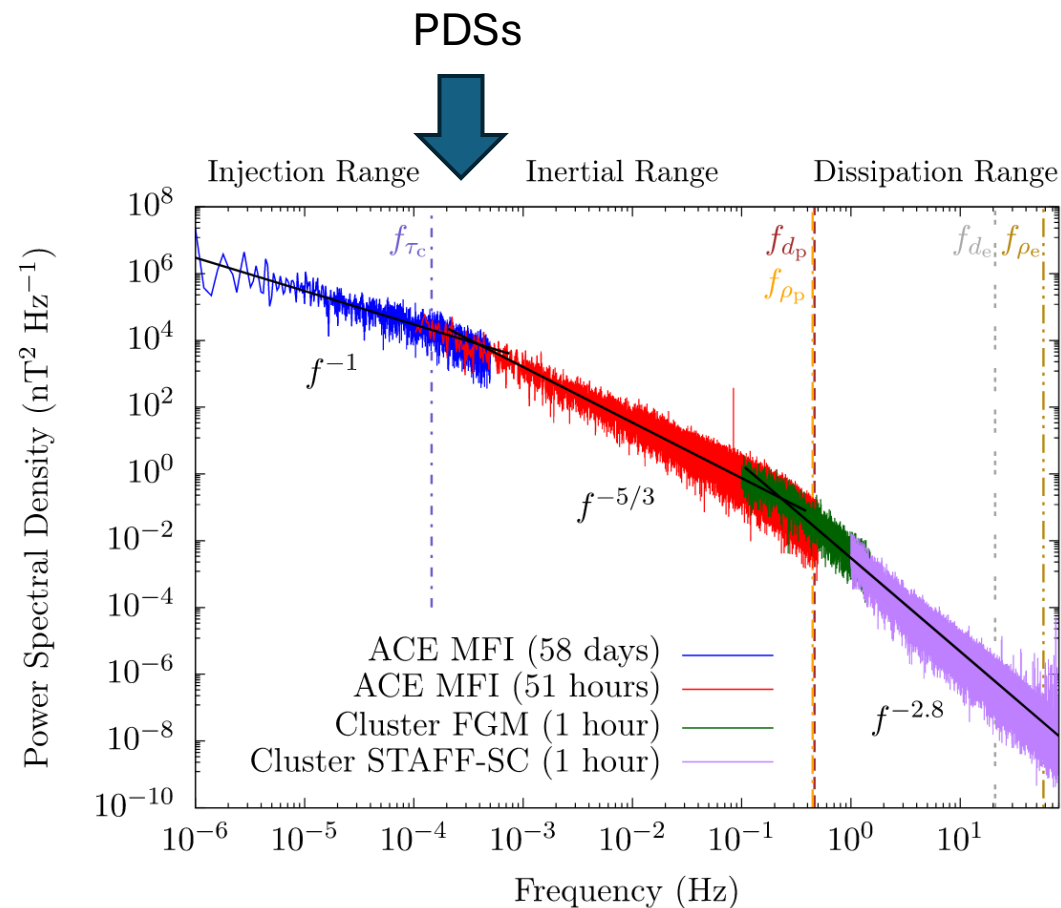
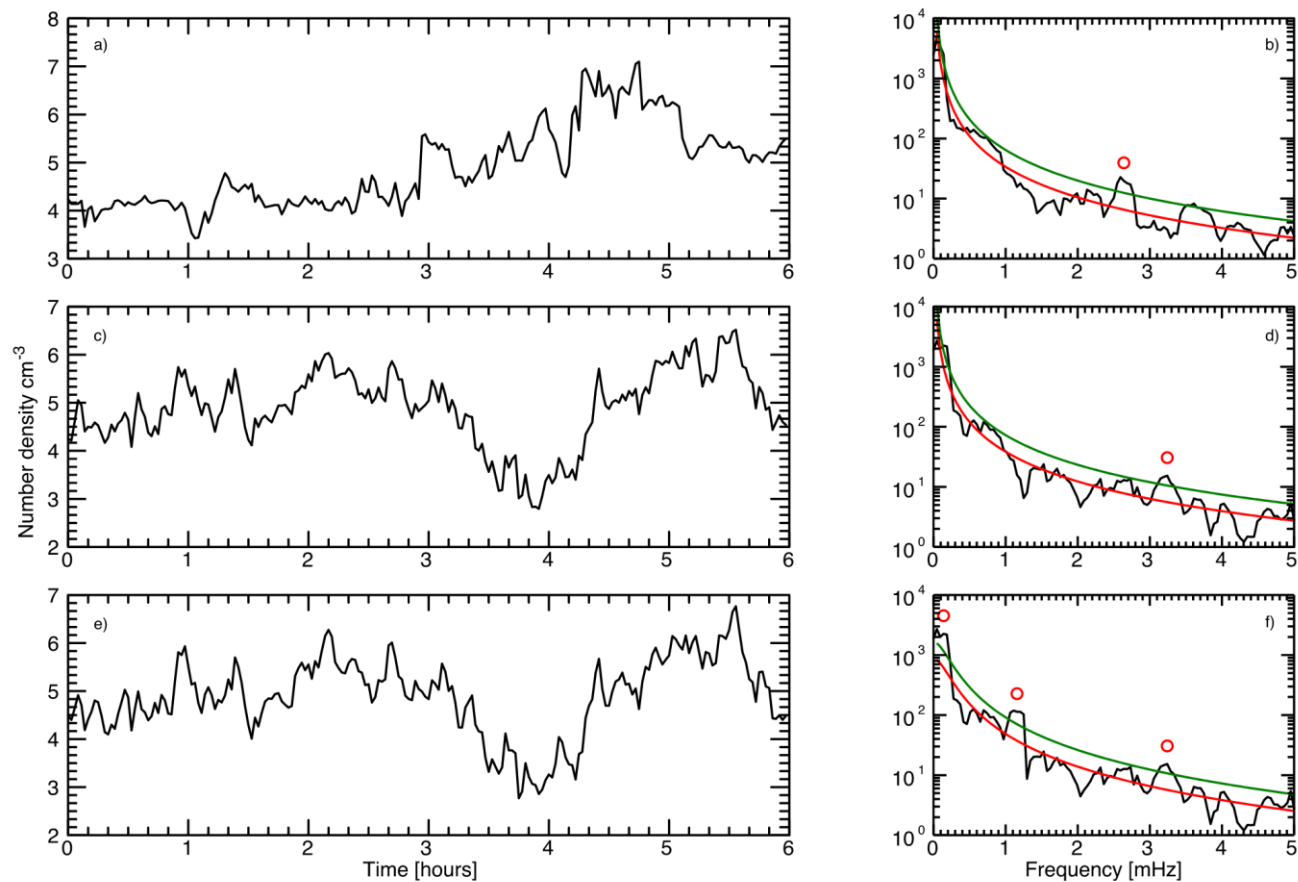


Study	Dataset(s)
● Slow Outflows	STEREO/EUVI, COR1, COR2
● Fast Outflows	STEREO/EUVI, COR1, COR2
— eq.(1) - Sheeley et al., 1997	SOHO/LASCO C2
- - eq.(2) - Sheeley et al., 1997; Jones & Davila, 2009	SOHO/LASCO C2; STEREO/COR1
■ Wang et al., 1998	SOHO/LASCO C2, C3
■ Song et al., 2009	SOHO/LASCO C3
■ Viall et al., 2010; Viall & Vourlidis, 2015	STEREO/COR2; HI-1
— Rouillard et al., 2010	STEREO/HI-1
■ DeForest et al., 2018	STEREO/COR2
■ Cho et al., 2018	SOHO/LASCO C3
■ Seaton et al., 2021	GOES-R/SUVI
■ Lopez-Portela et al., 2018	SOHO/LASCO C2, C3; STEREO/COR2
■ Lyu et al., 2024	STEREO/COR2
■ James, 1968	El Campo Antenna
— Woo, 1978	Helios 1/2; Pioneer 10/11
■ Tokumaru et al., 1991	Kashima 34-m Radio
■ Imamura et al., 2014	Akatsuki 8.4-GHz Radio
■ Efimov et al., 2018	Galileo S-Band Radio
■ Wexler et al., 2019	Helios; Messenger
■ eq.(22) - Wexler et al., 2020	Akatsuki 8.4-GHz Radio
— Frazin et al., 2003	SOHO/LASCO C2, UVCS

Periodic brightness variations related to OPDs remained in the range of 98 to 128 minutes, down to $\approx 2.0 R_s$.

Periodic Density Structures (PDSs) are solar wind density fluctuations from a few minutes to a few hours

Periodicity identified through spectral analysis techniques. Excess of power (red circle) at the 95% threshold (green line) above the background power (red line).

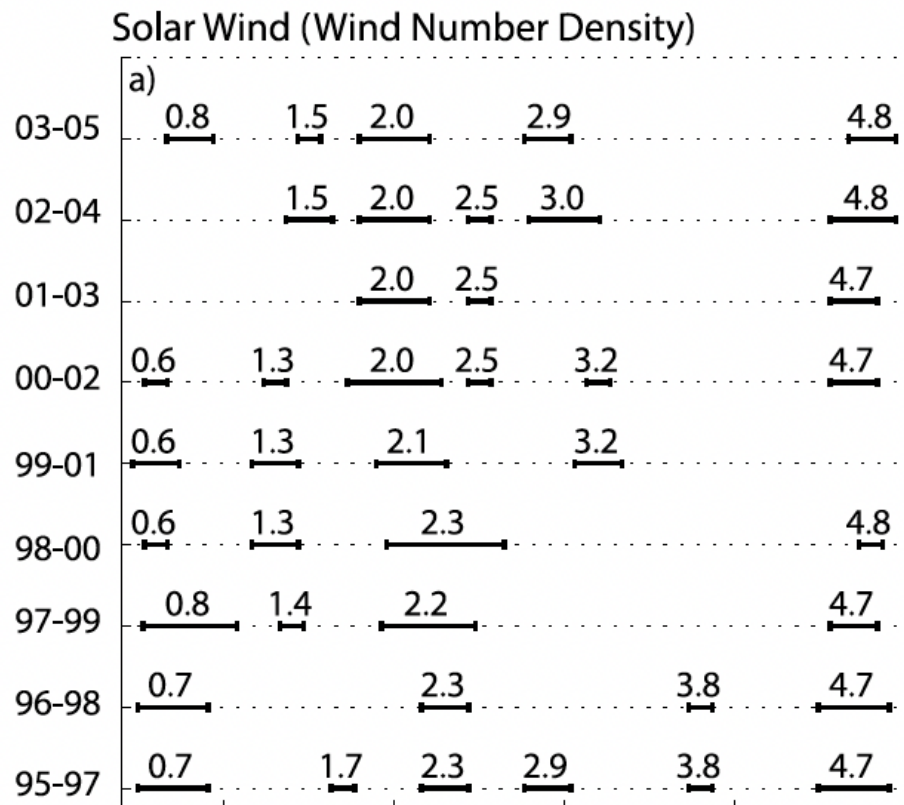


ACE MFI (58 days) — blue —
 ACE MFI (51 hours) — red —
 Cluster FGM (1 hour) — green —
 Cluster STAFF-SC (1 hour) — purple —

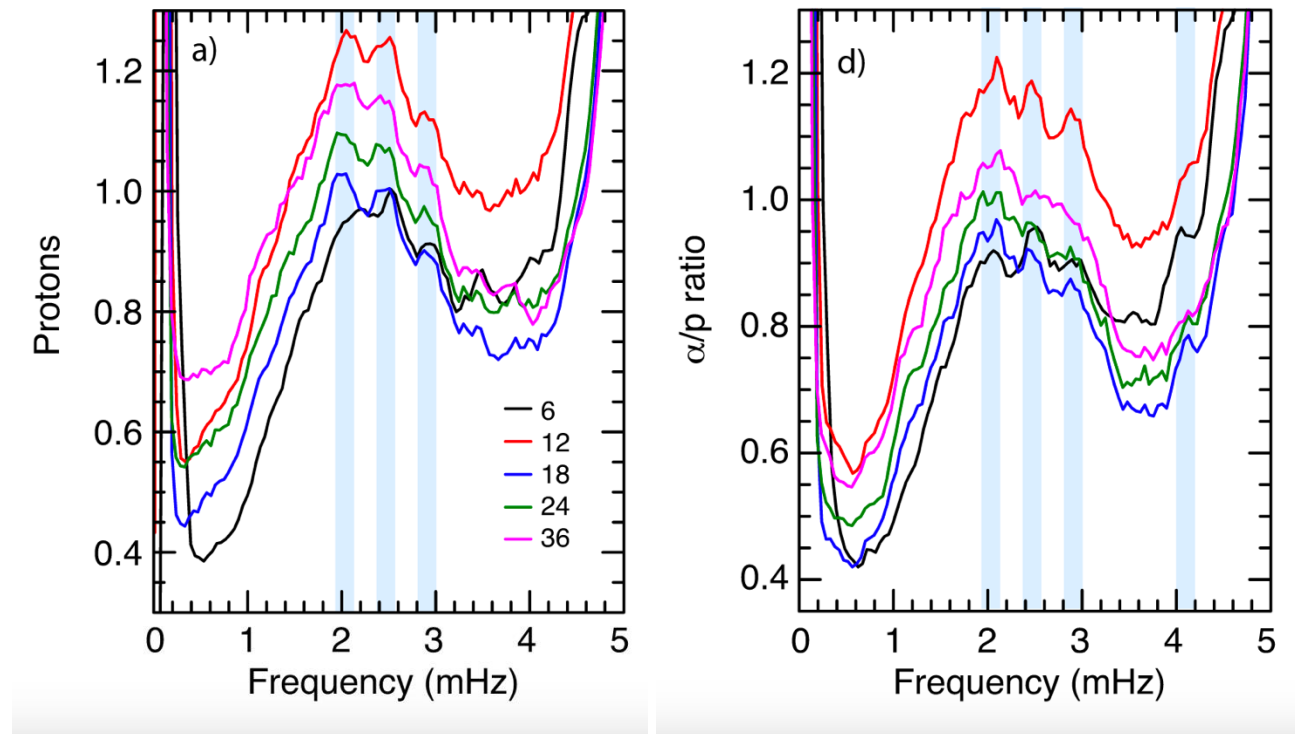
[Kiyani et al. \(2015\)](#)

The presence of periodicities is relevant in a statistical sense: There are more than we expect if PDSs were simply due to noise

Viall et al. (2009) conducted a long-term statistical analysis and found certain frequencies more frequent than others for fluctuations of the SW number density ($f \approx 0.7$, ≈ 1.4 , ≈ 2.0 , and ≈ 4.8 mHz).

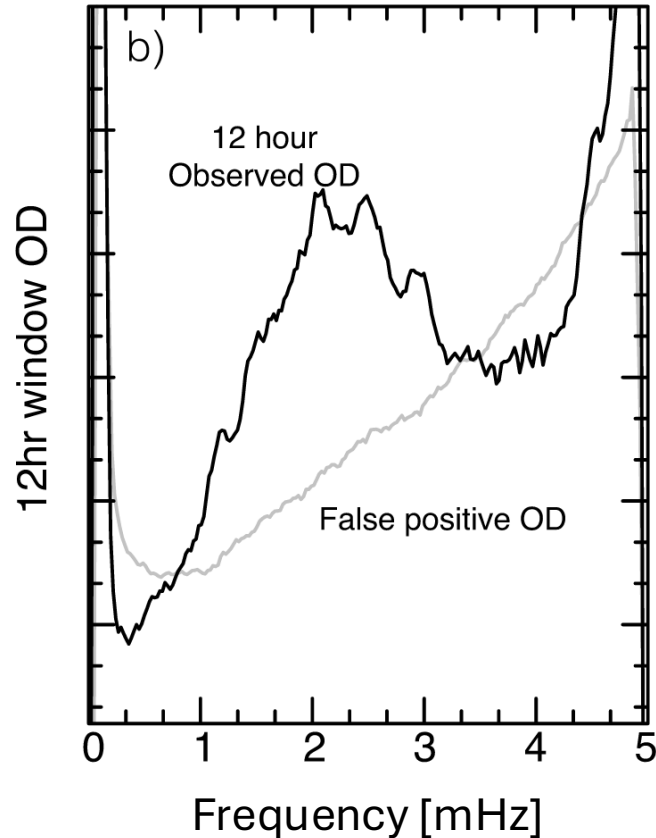


Similar analysis on more than 22 year of Wind data confirm the presence of PDSs

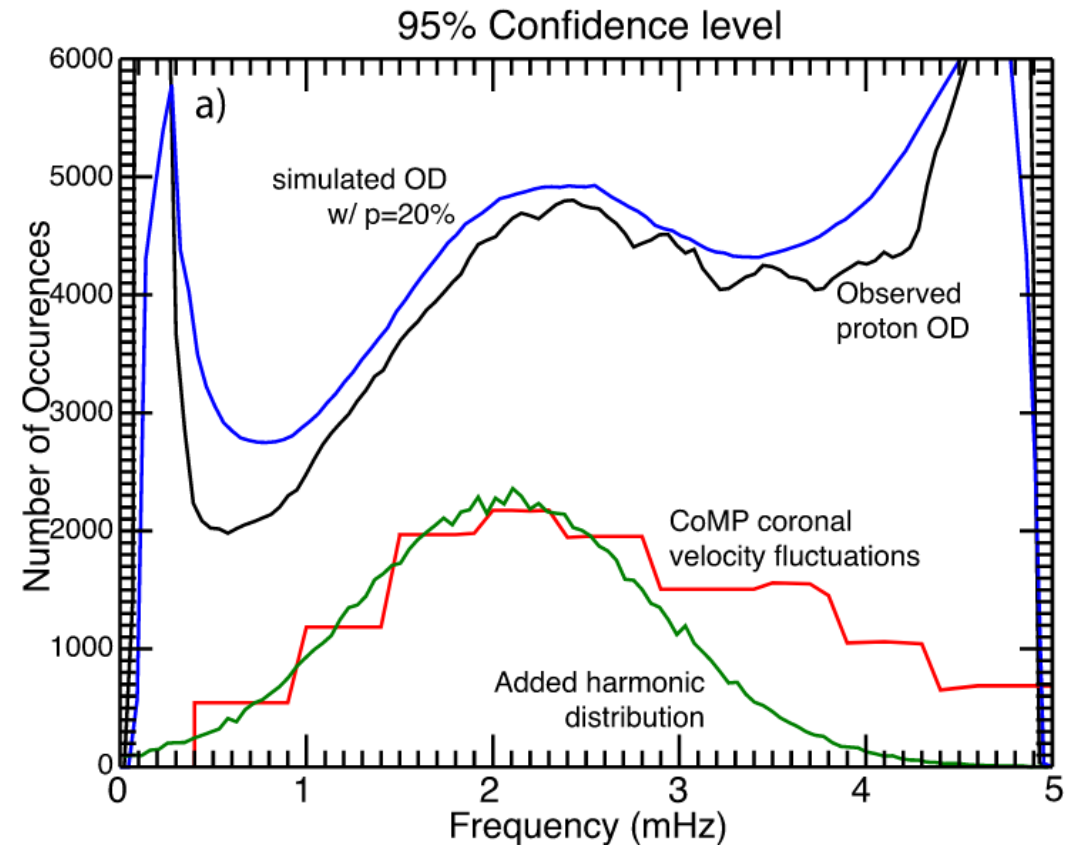


The presence of periodicities is relevant in a statistical sense: There are more than we expect if PDSs were simply due to noise

Forward modeling of red noise spectra, simulating turbulence, does not reproduce the occurrence distribution (OD) of PDSs.



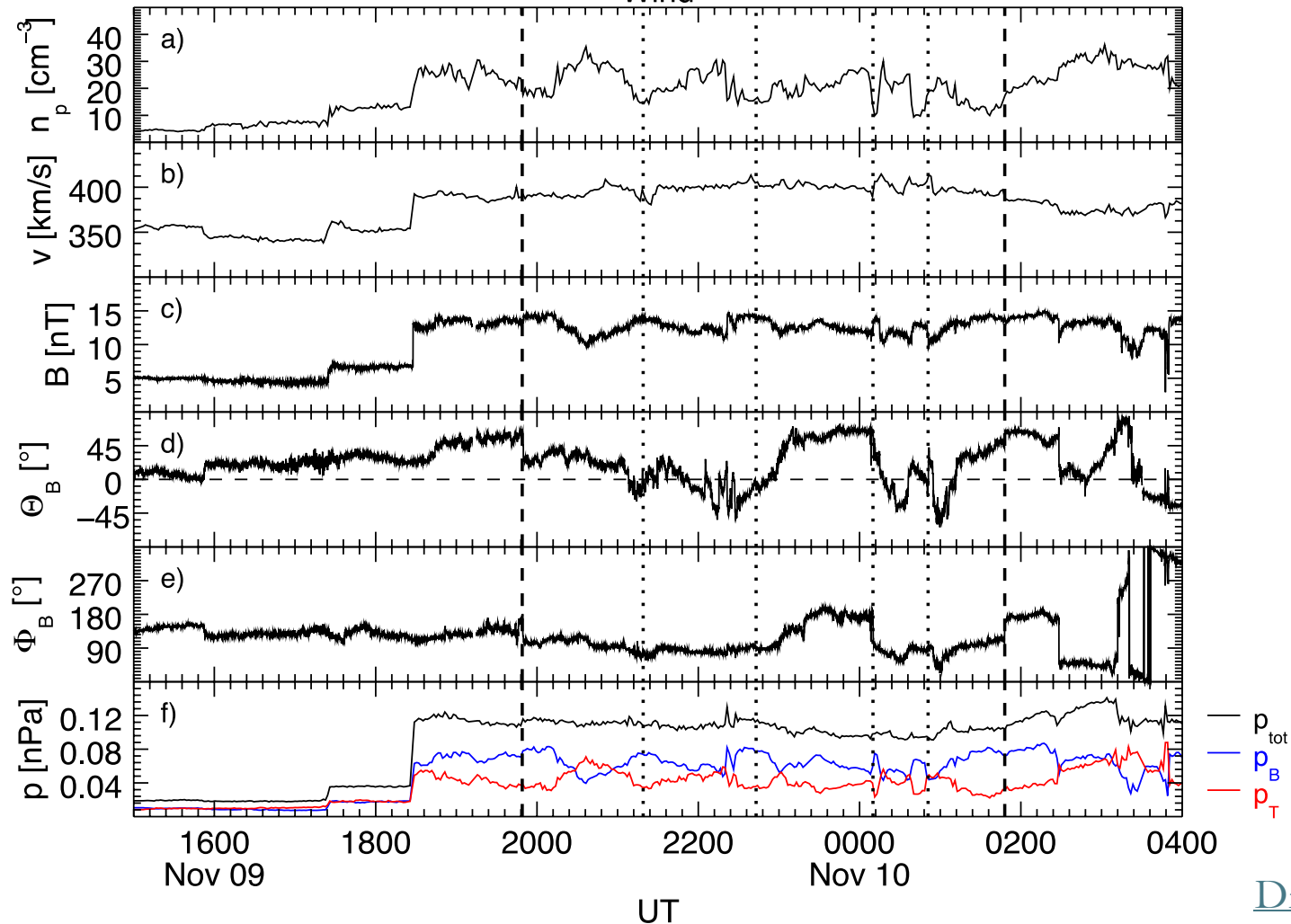
The occurrence distribution (OD) can be reproduced if we account for the presence of PDSs (green profile) in the solar wind. Red lines is the OD of transversal velocity fluctuations in the corona.



Can we characterize the associated plasma and magnetic field properties?

Wind at 1 AU

≈ 90 ≈ 84 ≈ 87 ≈ 41 ≈ 57 min
Wind



Black lines delimit five PDSs

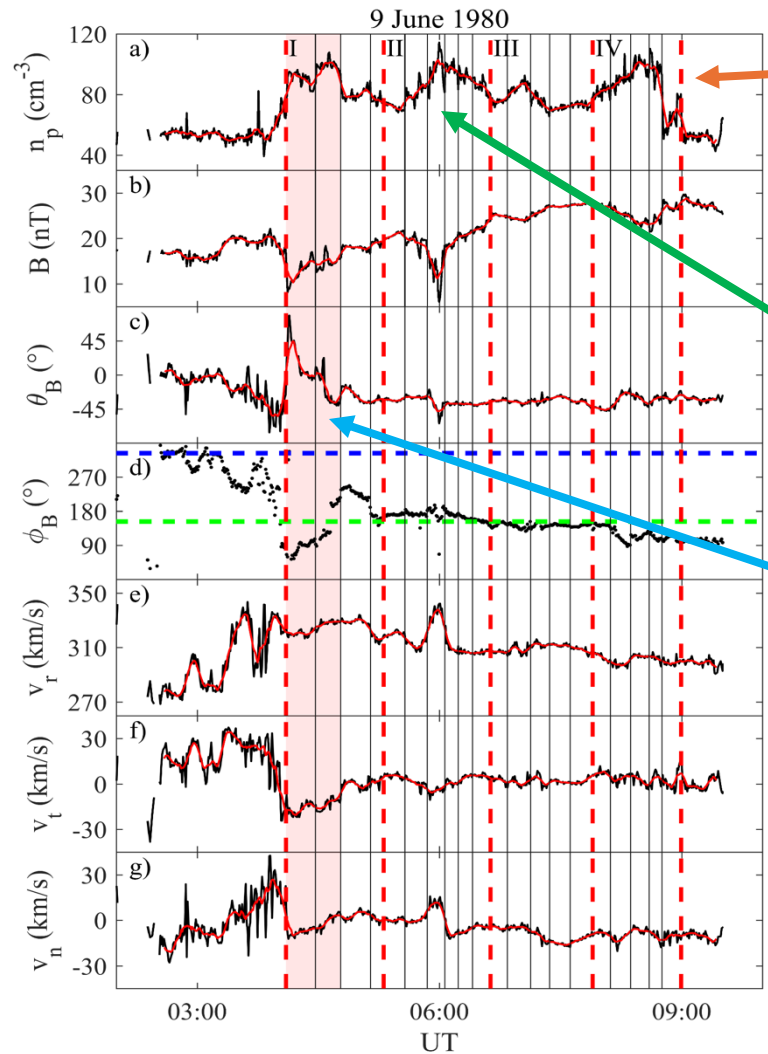
Observed more often in slow solar wind streams

Sometimes delimited by interplanetary magnetic field discontinuities

PDSs are in pressure balance and advect with the solar wind

Evidence in support of the solar origin of PDSs

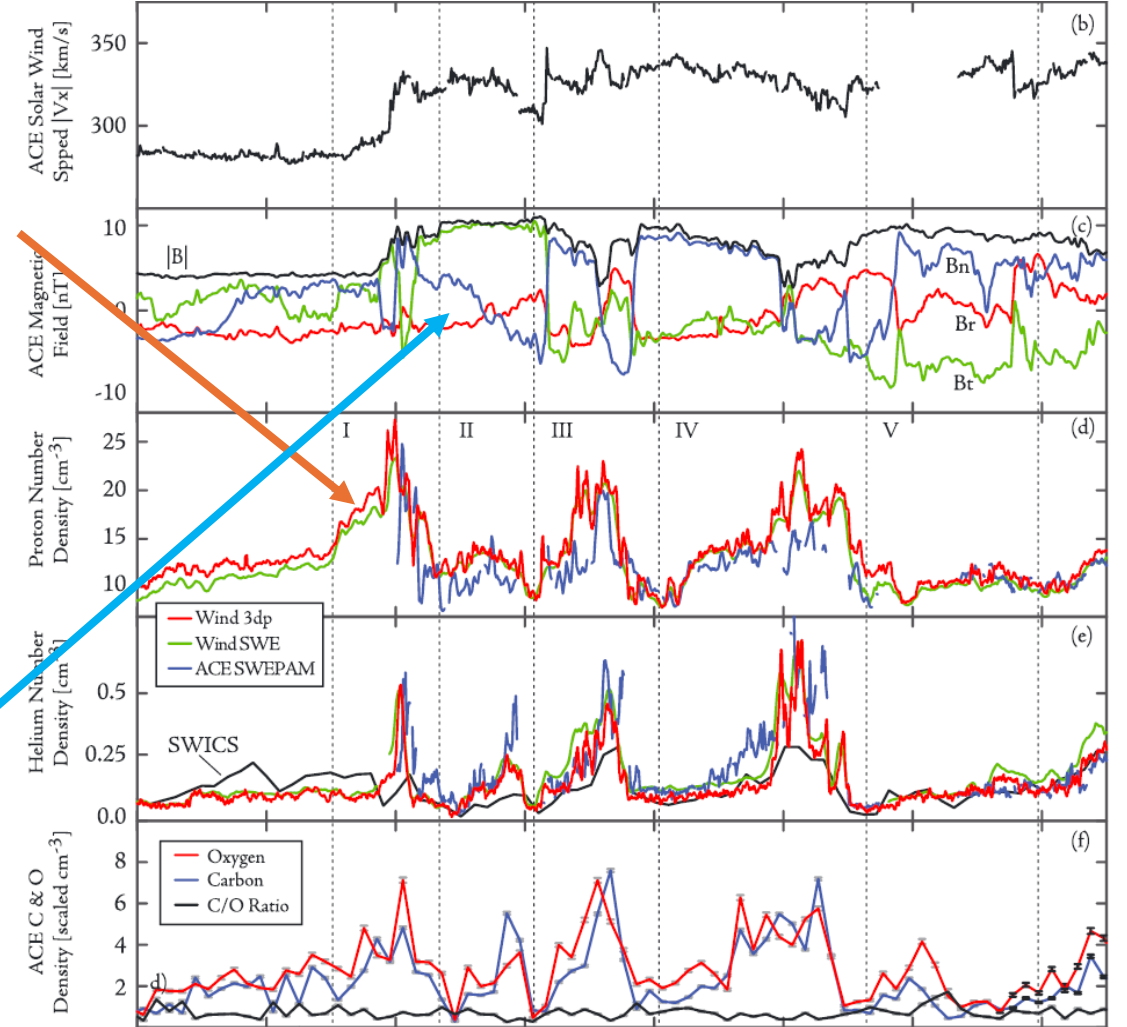
Helios probe observations of PDSs at ≈ 0.4 AU (Di Matteo et al., 2019).



Density Structures with ≈ 90 min periodicities

Additional periodicities at ≈ 29 min (≈ 0.57 mHz) and ≈ 11 min (≈ 1.55 mHz)

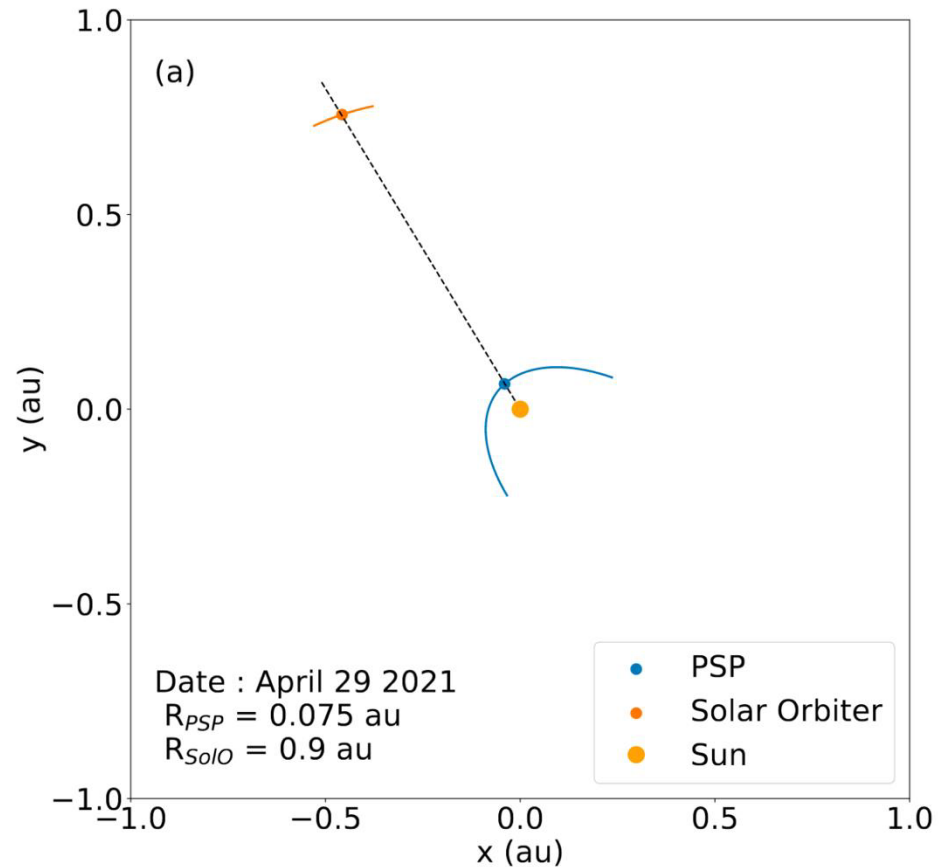
Evidence of magnetic flux-ropes



Proton density changes and changes in alphas, C, and O at ≈ 1 AU support their solar origin! (Kepko et al., 2016)

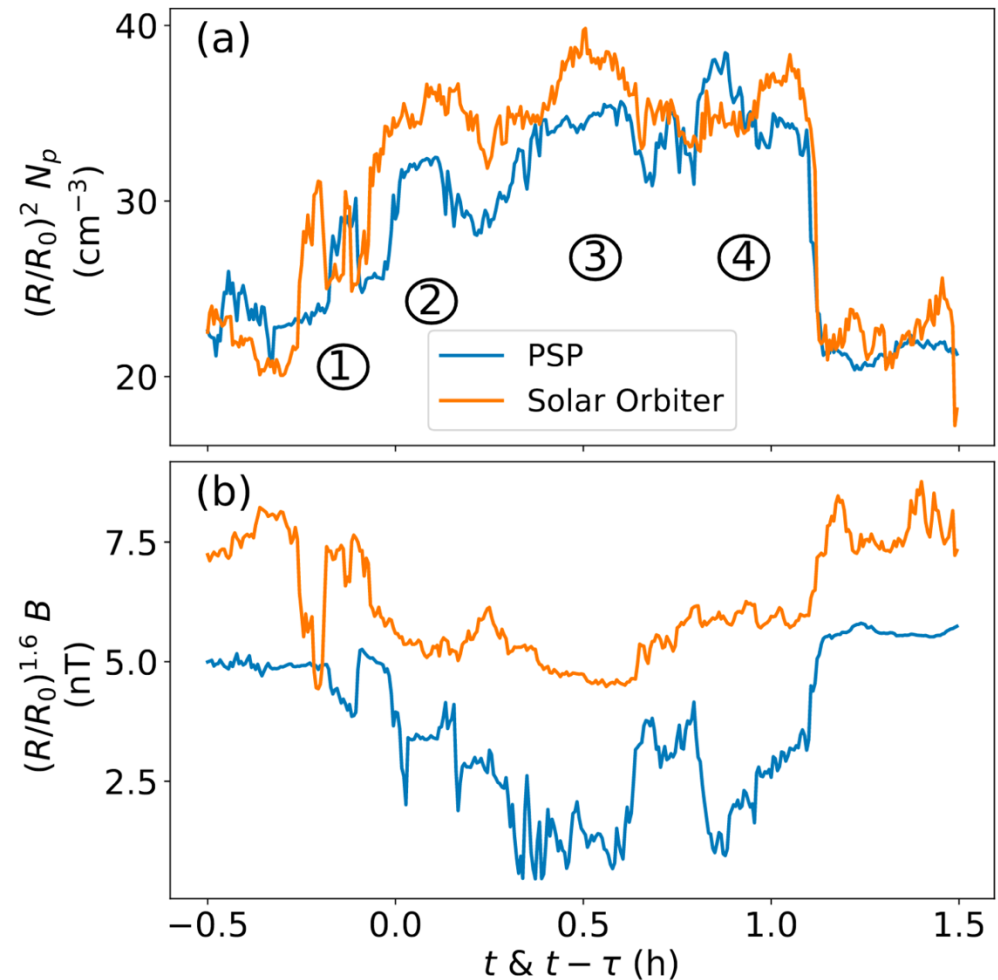
Can structures formed at the Sun survive out to 1 AU?

Radial alignment of Parker Solar Probe and Solar Orbiter



[Berriot et al. \(2024\)](#)

Scaled density and magnetic field at the two spacecraft

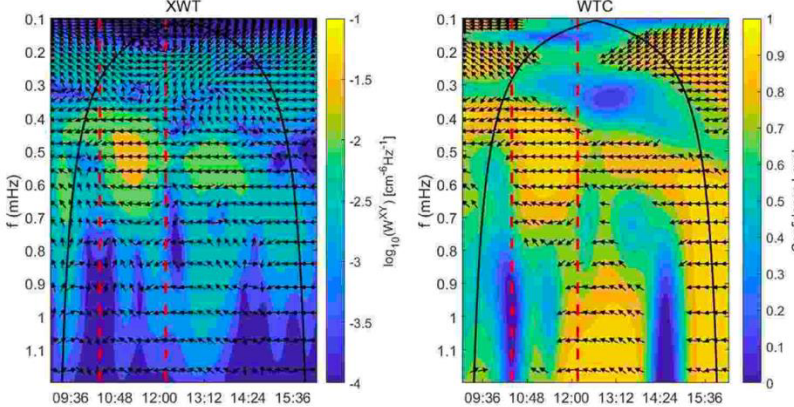
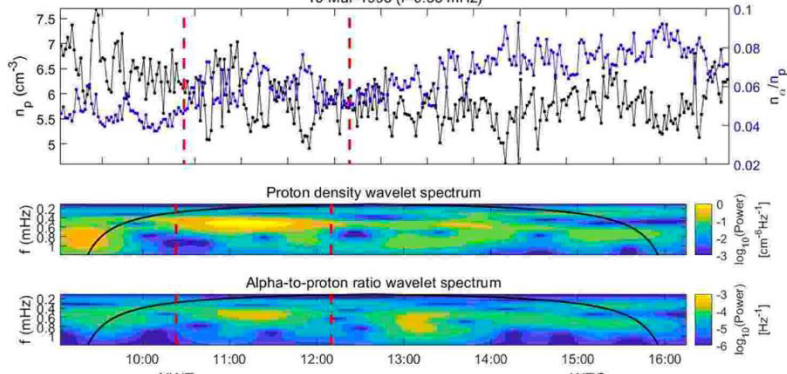


The thermodynamic properties of some PDSs (“coherent” PDS) support their association with flux ropes

We explored the polytropic index for “coherent” and “incoherent” PDSs

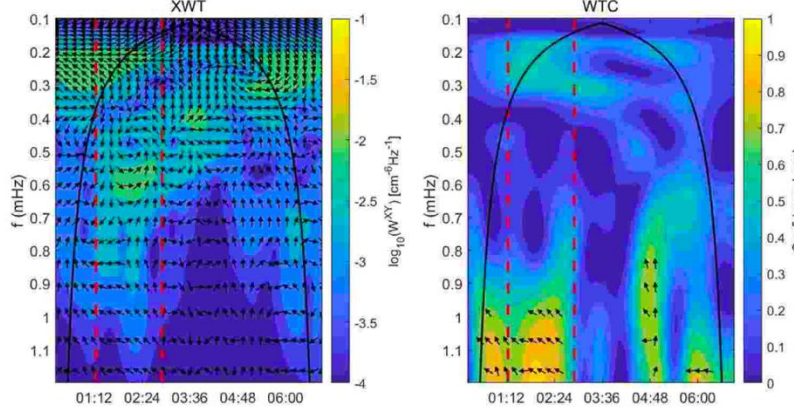
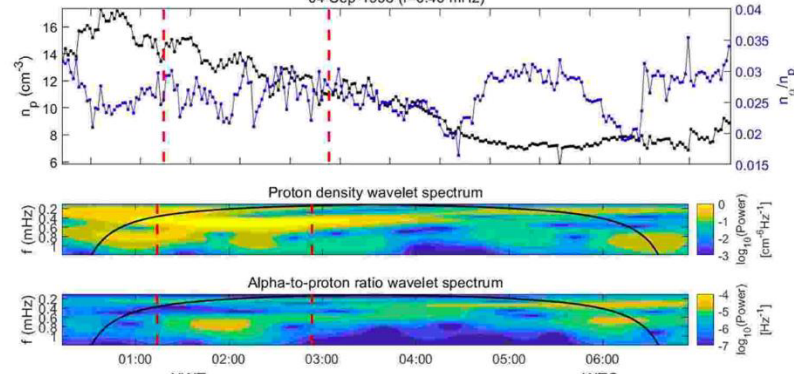
Example of coherent event

10-Mar-1995 (f=0.53 mHz)



Example of incoherent event

04-Sep-1998 (f=0.46 mHz)



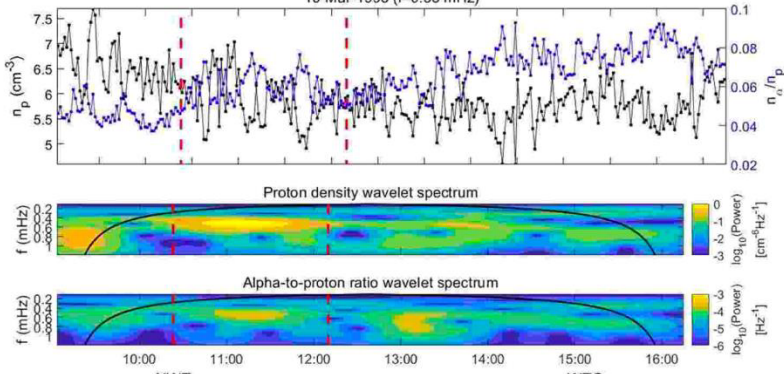
The thermodynamic properties of some PDSs (“coherent” PDS) support their association with flux ropes

We explored the polytropic index for “coherent” and “incoherent” PDSs

- The thermodynamic evolution in 336 interplanetary coronal mass ejections (ICMEs) using approximately 20 years of Wind data show that ejecta (ICME flux rope) exhibited an average $\gamma \approx 1.54$ (Dayeh & Livadiotis, 2022).
- Our result for the coherent PDS events is the same, i.e., $\gamma \approx 1.54$.

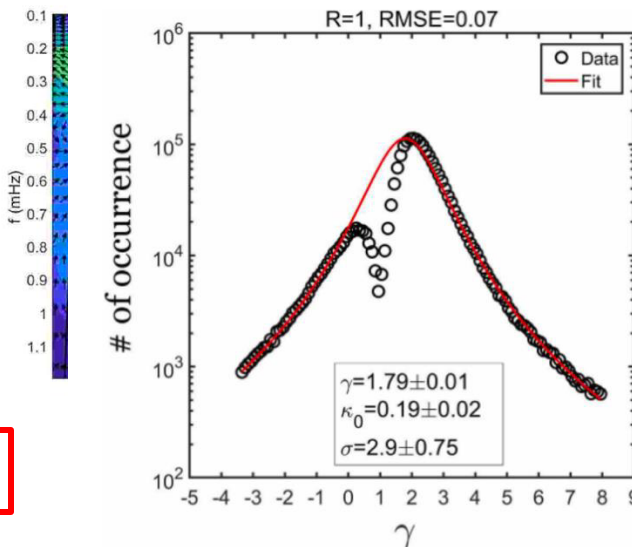
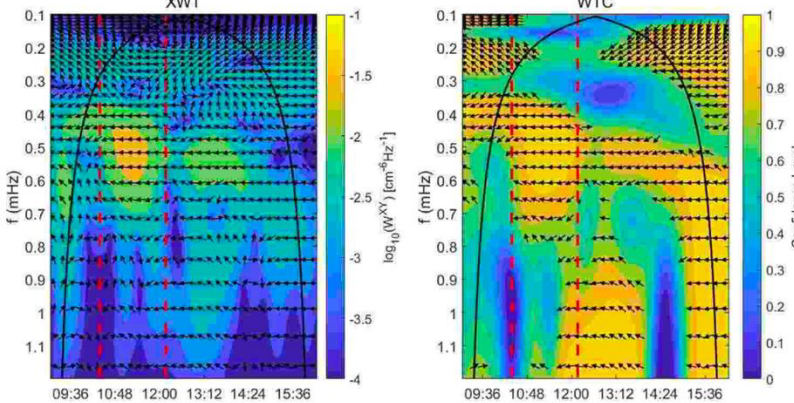
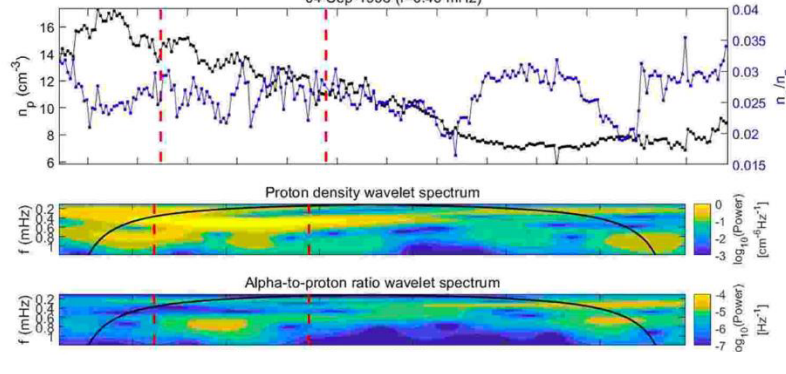
Example of coherent event

10-Mar-1995 (f=0.53 mHz)

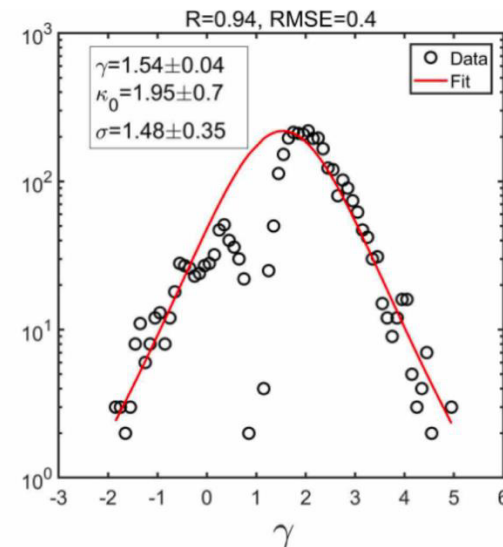


Example of incoherent event

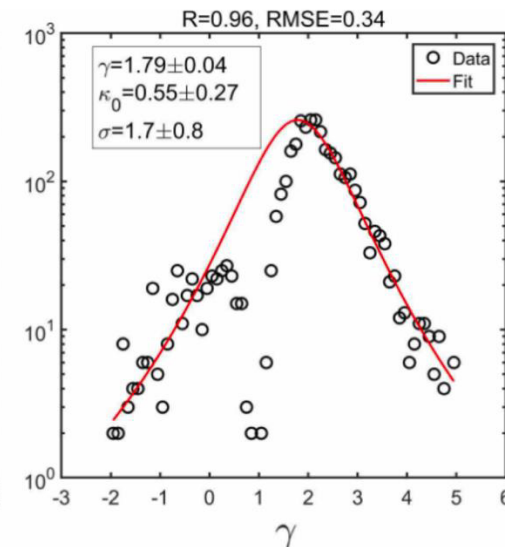
04-Sep-1998 (f=0.46 mHz)



All SW



Coherent PDS



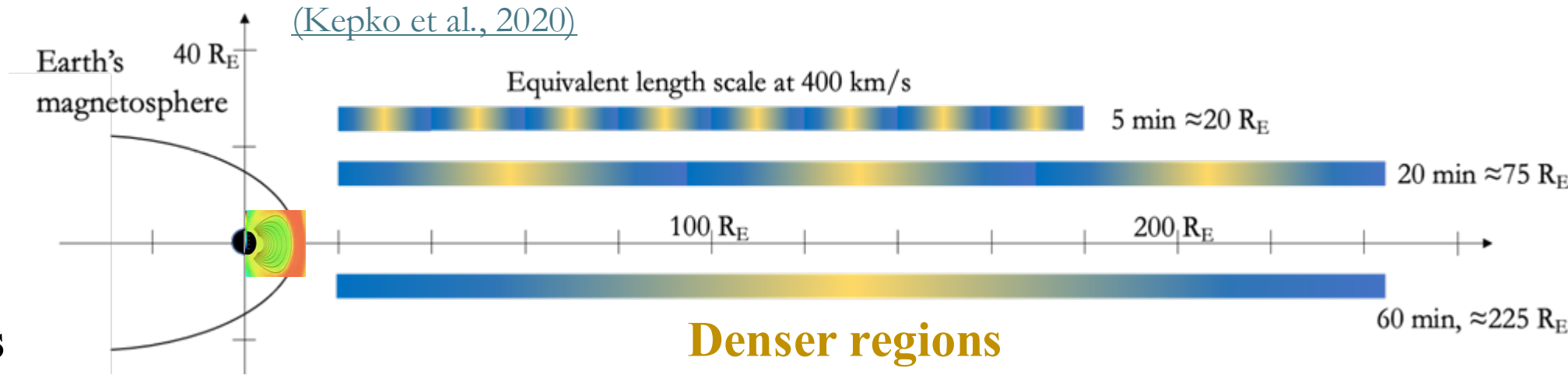
Incoherent PDS

$$\ln T_p = (\gamma - 1) \cdot \ln n_p + \text{const.}$$

Radial Length Scales from tens to few thousands Earth's radii (R_E)

**PDSs size scales
unknown in the
perpendicular
direction**

Radial size scales

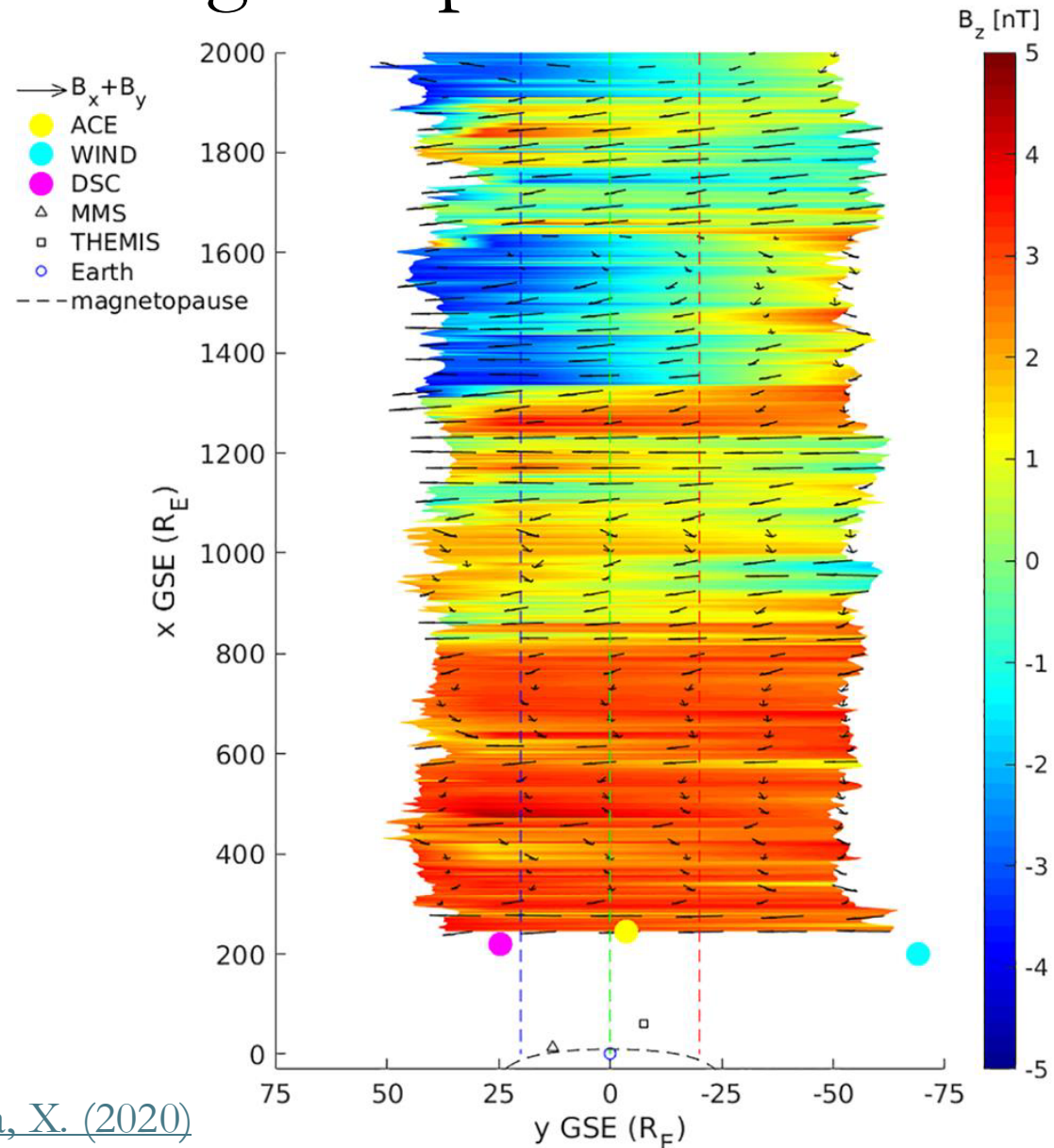


What is the azimuthal extent of PDSs?

- 1) Guide assumptions of magnetosphere upstream condition affecting interpretation of solar-wind/magnetosphere coupling ([Burkholder et al. 2020](#); [Di Matteo and Sivadas, 2022](#)).
- 2) Pose constraints for theories that aim to explain the origin of PDSs.

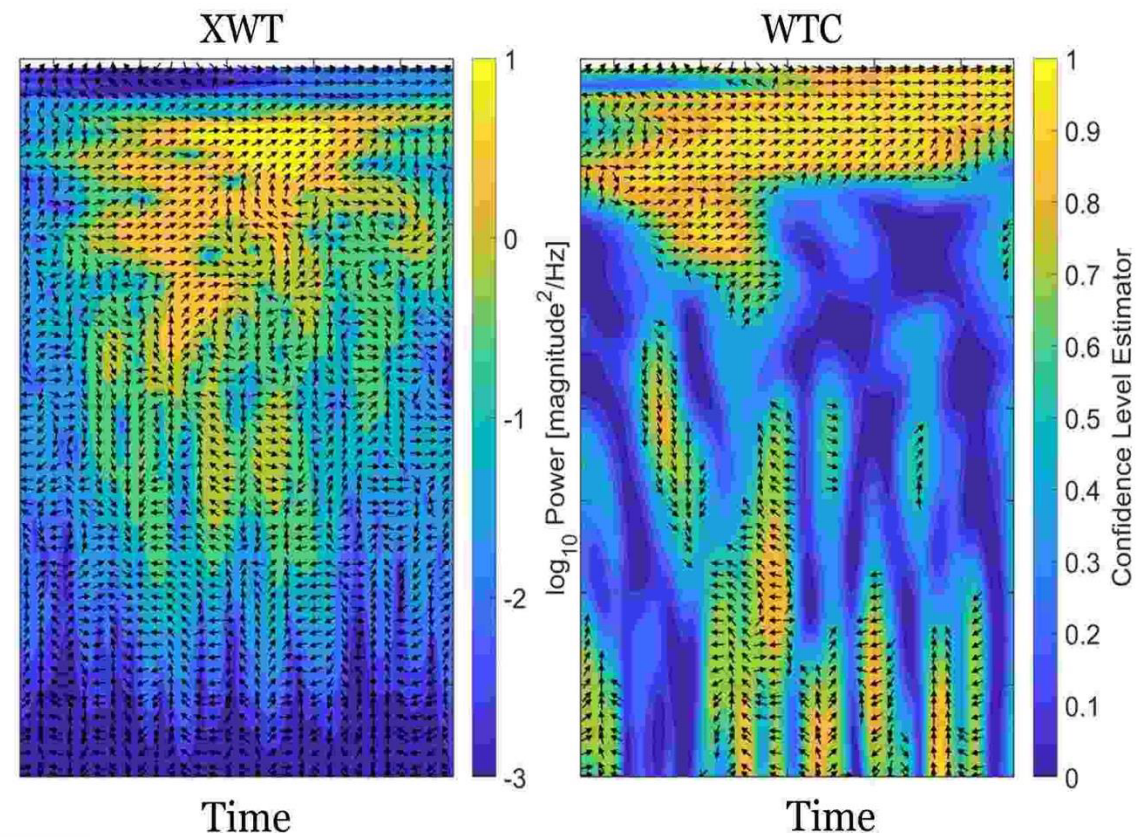
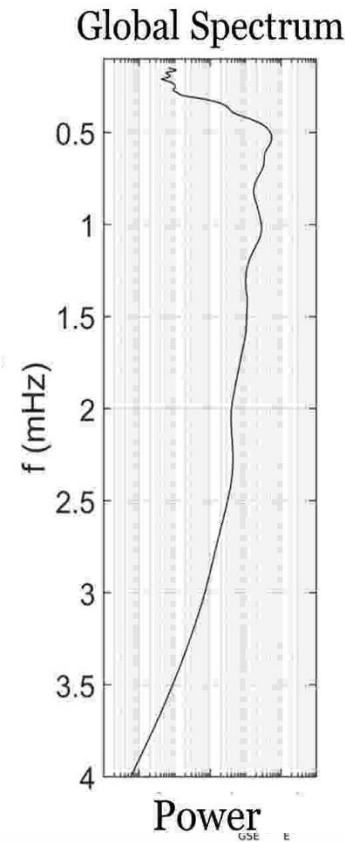
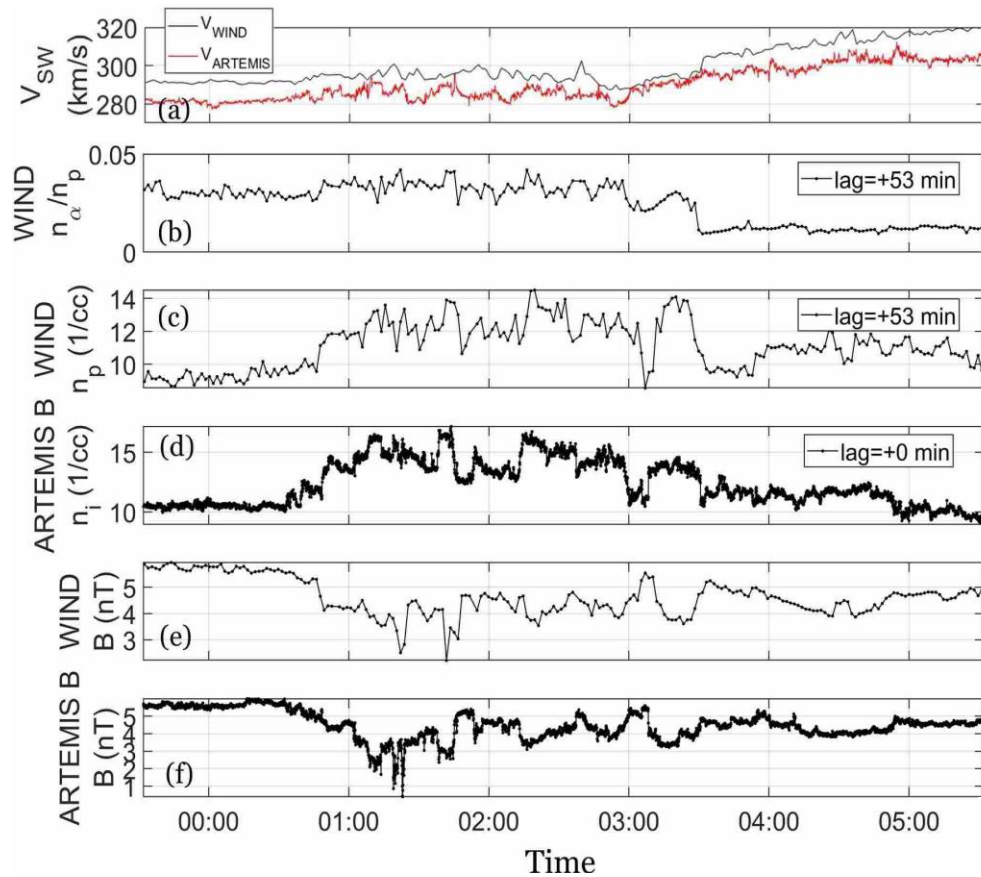
Gradients in the solar wind on scale sizes of the same order of the magnetosphere dimension

- ❑ Keep in mind possible gradients in solar wind upstream conditions when interpreting magnetosphere response
- ❑ Multispacecraft monitor shows improvement in predictions for 44% of the cases over single-spacecraft (OMNI dataset) predictions ([Burkholder et al., 2020](#))



We leverage the periodic nature of the PDSs to perform coherence analysis from observations at two spacecraft

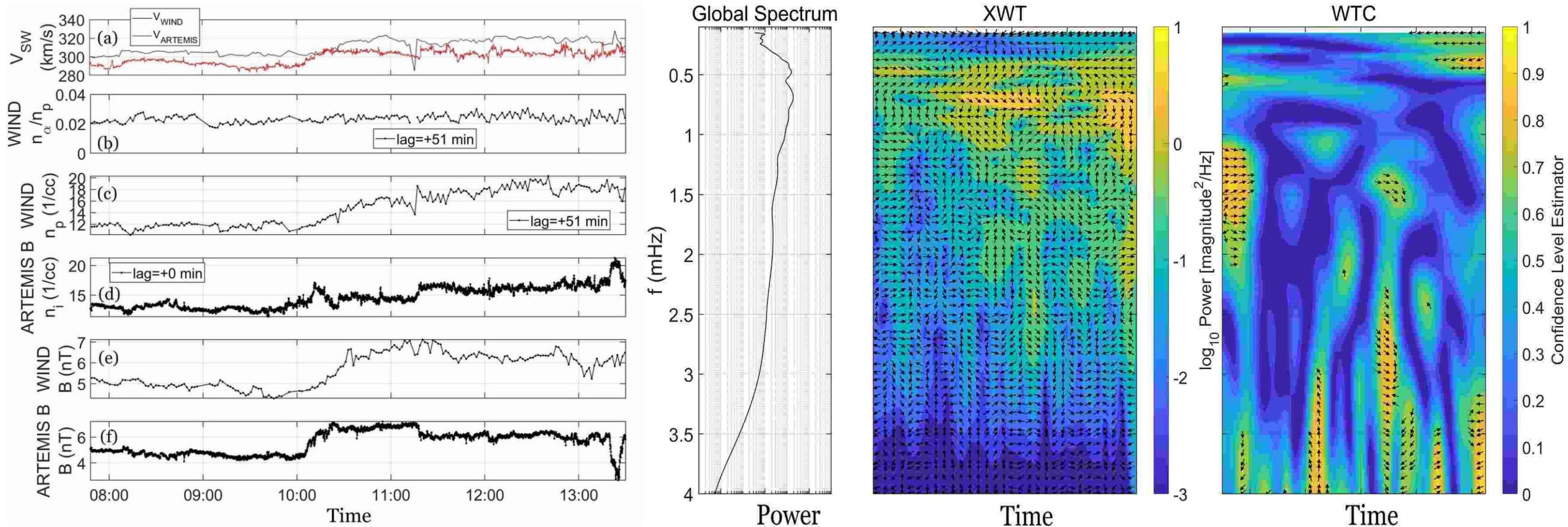
[Di Matteo et al. \(2024\)](#)



Example of high coherence PDSs at ≈ 0.6 mHz, July 8, 2013

We leverage the periodic nature of the PDSs to perform coherence analysis from observations at two spacecraft

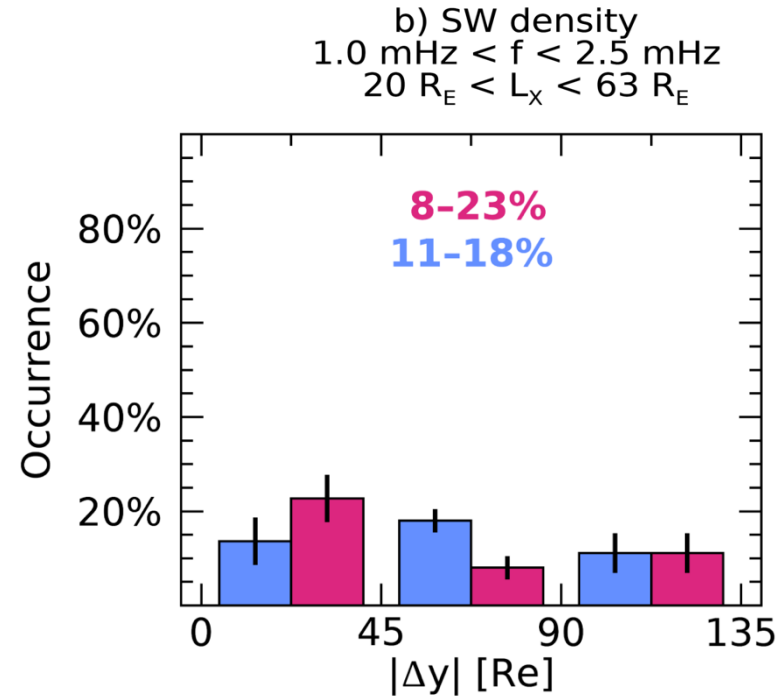
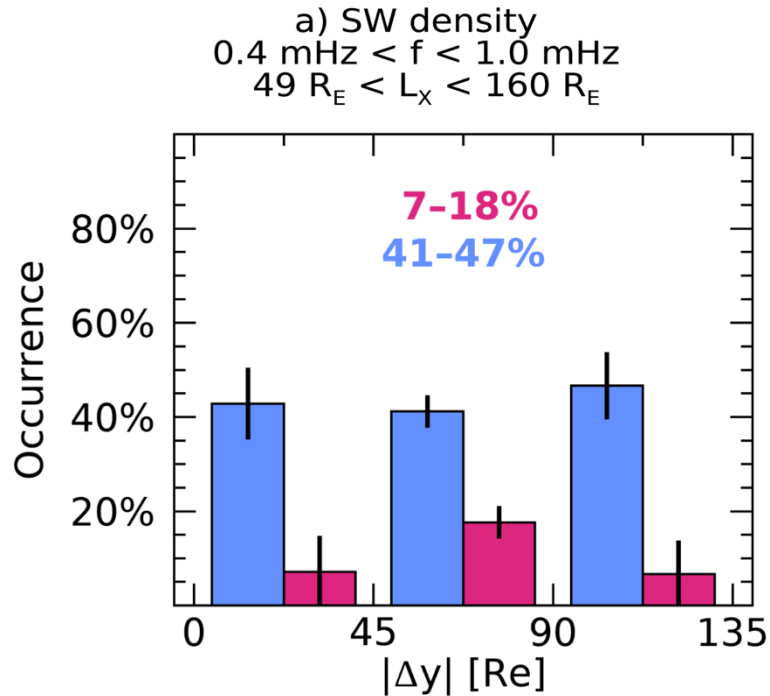
[Di Matteo et al. \(2024\)](#)



Example of low/no coherence PDSs at ≈ 0.6 mHz July 9, 2013

Coherence rate dependence on spacecraft location appears to be mainly regulated by separation along the Y_{GSE} direction.

[Di Matteo et al. \(2024\)](#)



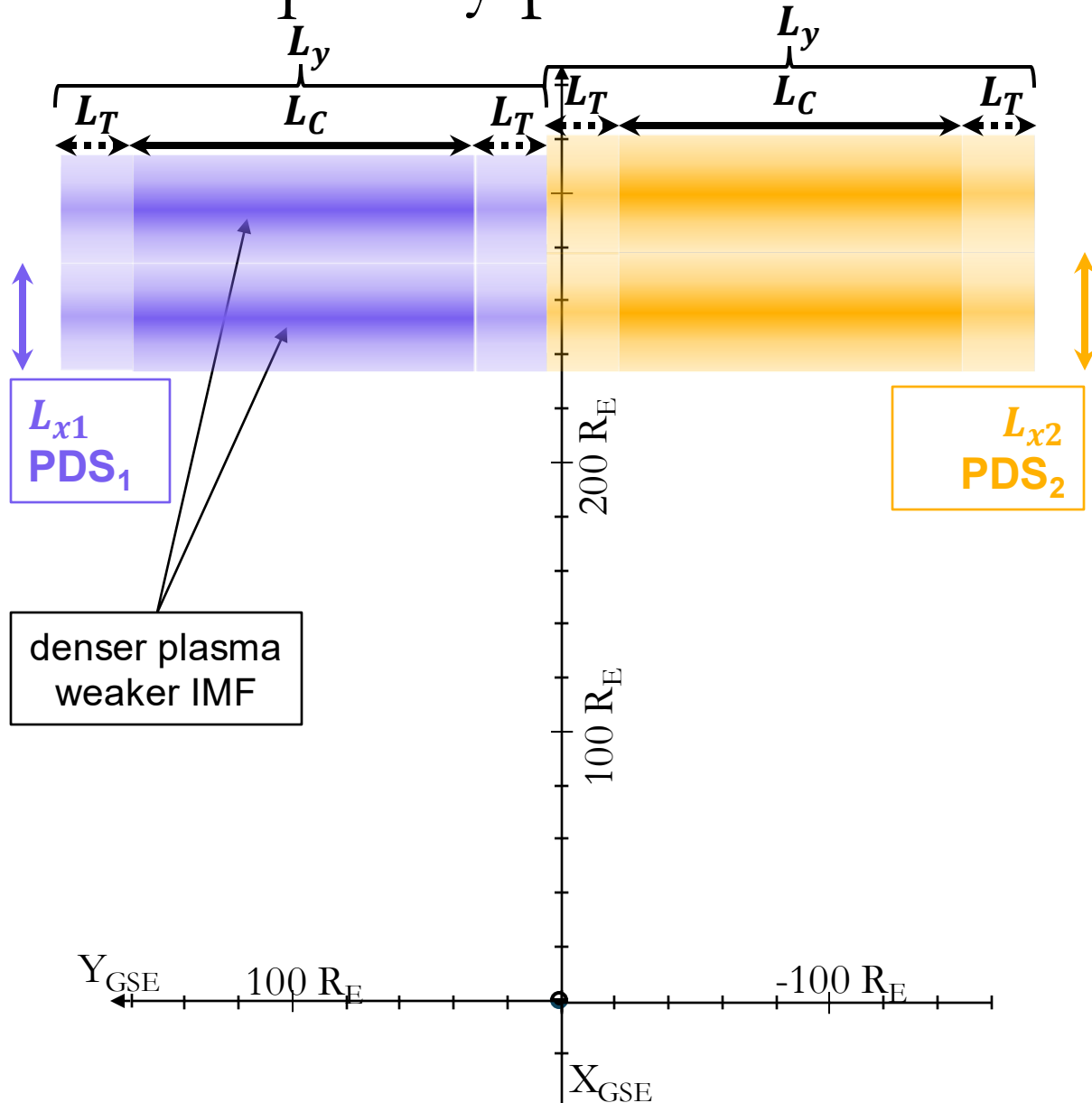
- **High coherence PDSs:** $|f_W - f_A| < 3\Delta f$ and $WTC \geq 0.7$ continuously for more than two periods of the PDS
- **Low/no coherence PDSs:** $|f_W - f_A| < 3\Delta f$ but WTC criterium not satisfied

Hypotheses

The occurrence rates saturate for small $|\Delta Y_{GSE}|$ and are non-zero up to the larger $|\Delta Y_{GSE}|$, suggesting that:

- 1) The azimuthal scale of PDSs is at least larger than the maximum separation of the two spacecraft, that is $|\Delta Y_{GSE}| \approx 130 R_E$
- 2) The actual PDS azimuthal scale might be regulating the saturation values of the occurrence rates.

We developed a simple forward model to test our hypotheses and consequently provide estimates of the PDSs azimuthal scales.



[Di Matteo et al. \(2024\)](#)

Schematic representation to scale of the simulation setup depicting the transit of PDSs at the spacecraft locations.

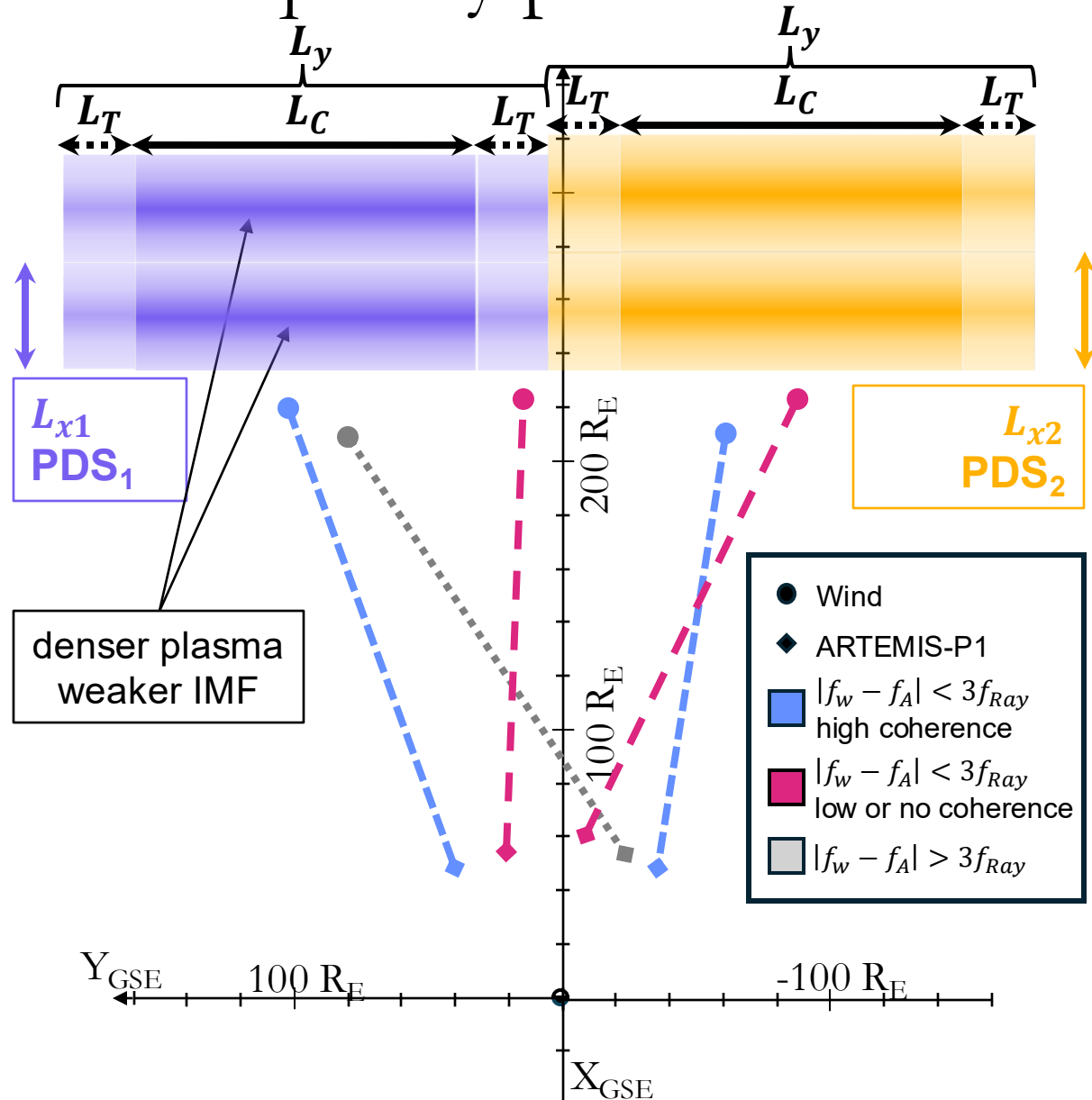
Purple and **yellow** stripes represent structures at different frequency/radial length scale.

The **dark** and *light* areas indicate the **high** and *low/no* coherence regions of azimuthal scale L_C and L_T , respectively.

The azimuthal extent of PDS is

$$L_y = L_C + 2L_T$$

We developed a simple forward model to test our hypotheses and consequently provide estimates of the PDSs azimuthal scales.



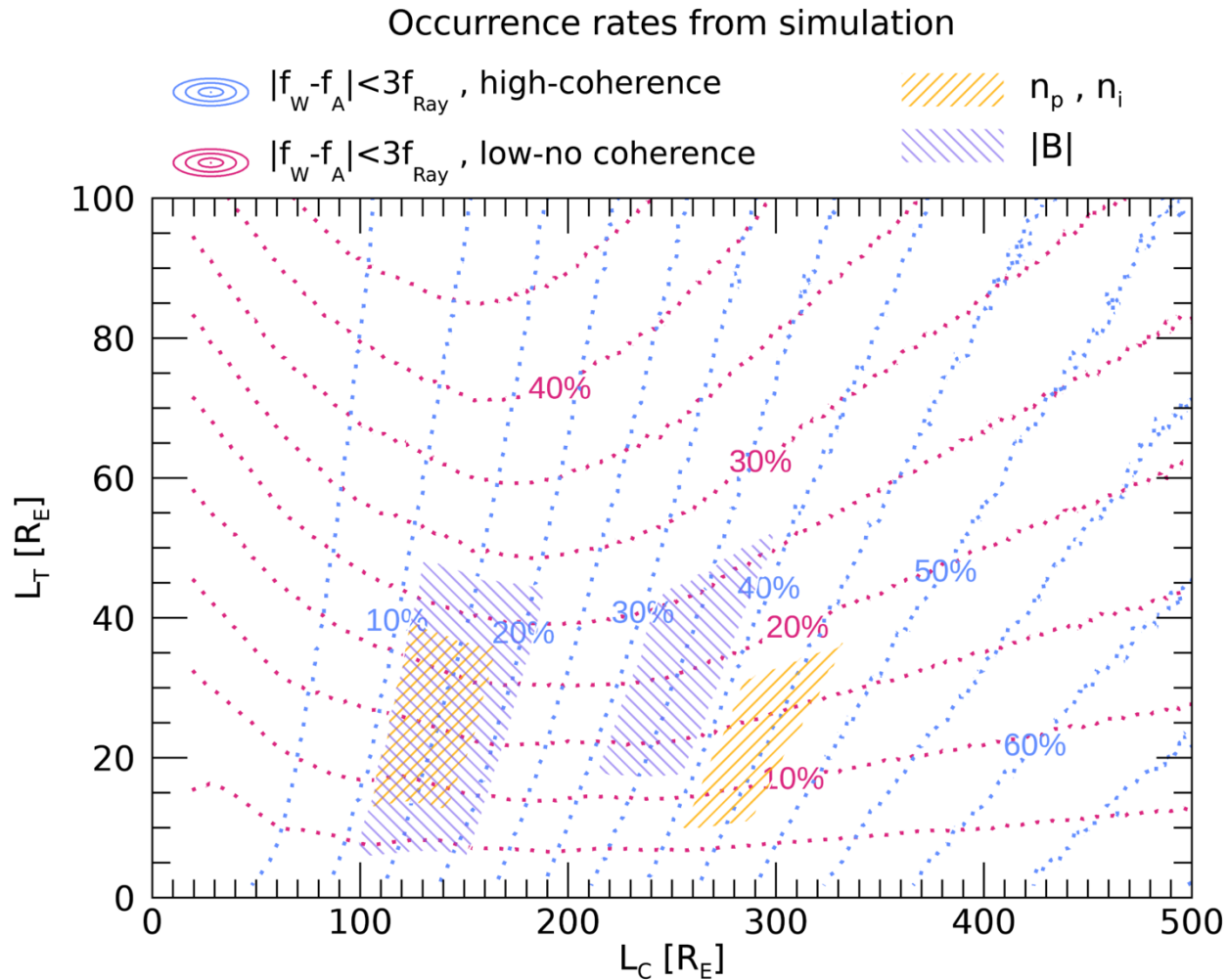
[Di Matteo et al. \(2024\)](#)

Connected circles and diamonds show possible spatial configuration of Wind and ARTEMIS-P1.

Colors indicate the corresponding expected outcome of the spectral plus coherence analysis, considering only the $|\Delta Y_{GSE}|$ spacecraft separation, namely:

- **same PDSs with high coherence**
- **same PDSs with low/no coherence**
- **different PDSs**

Observed occurrence rate of high and low/no coherence events determine that PDS have a finite azimuthal extent



[Di Matteo et al. \(2024\)](#)

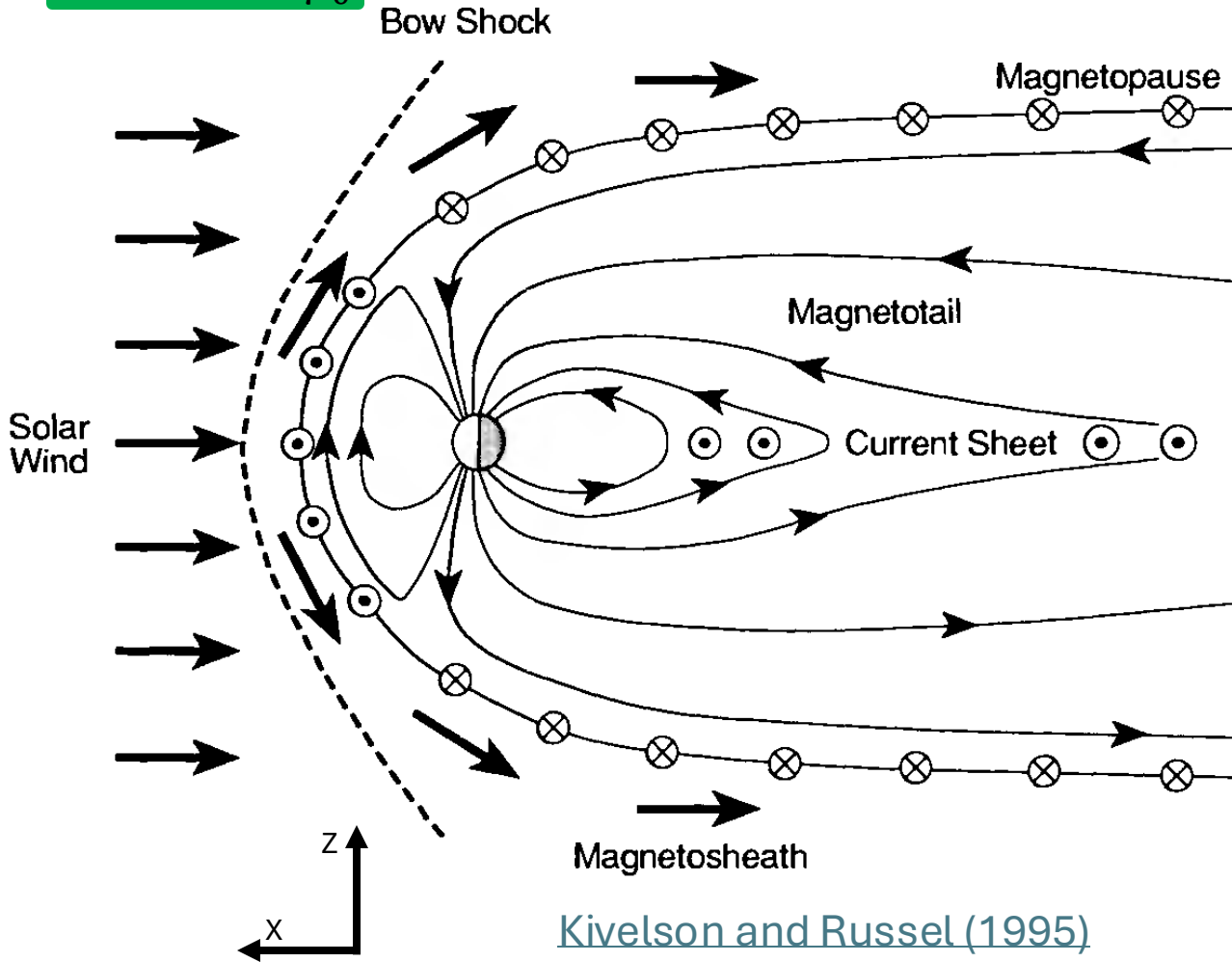
Occurrence rate contour levels for PDSs with high (blue) or low/no (magenta) coherence obtained by 10,000 simulations of PDS transit at the actual spacecraft location for each combination of L_C and L_T .

Striped **yellow** and **purple** areas cover the occurrence rates observed in **solar wind density** and **IMF intensity**.

Parameter	L_x	L_C	L_T	L_y
	[R_E]	[R_E]	[R_E]	[R_E]
n_p, n_i	86^{+74}_{-37}	294 ± 39	23 ± 14	340 ± 67
$ B $	88^{+64}_{-35}	256 ± 43	35 ± 18	326 ± 79
n_p, n_i	35^{+28}_{-15}	135 ± 30	26 ± 13	187 ± 56
$ B $	34^{+34}_{-14}	144 ± 45	27 ± 21	198 ± 87

PDSs can directly drive magnetospheric field fluctuations treated as quasi-static modulation of the magnetosphere

$$n_p m_p u_x^2 \approx \frac{B_z^2}{2\mu_0}$$

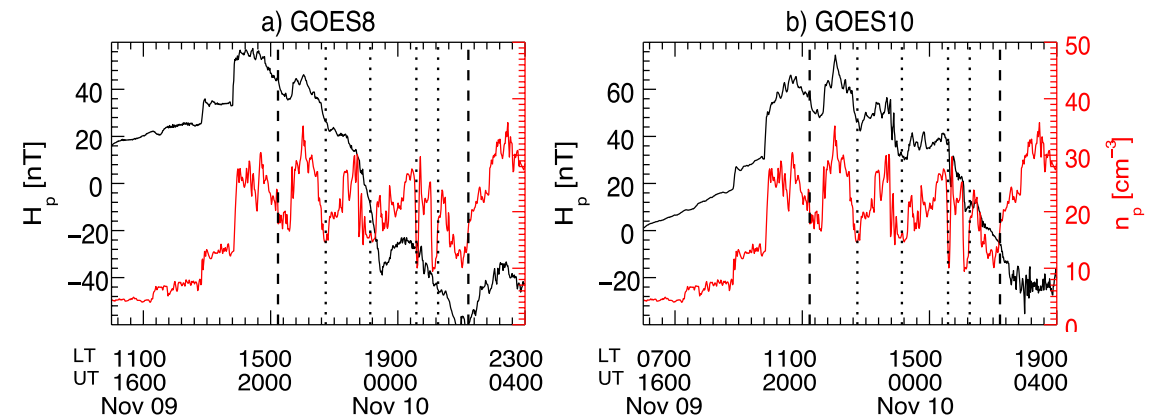


[Kivelson and Russel \(1995\)](#)

≈ 0.2 1 2 3 4 mHz

PDSs driven

Pc5 ULF waves

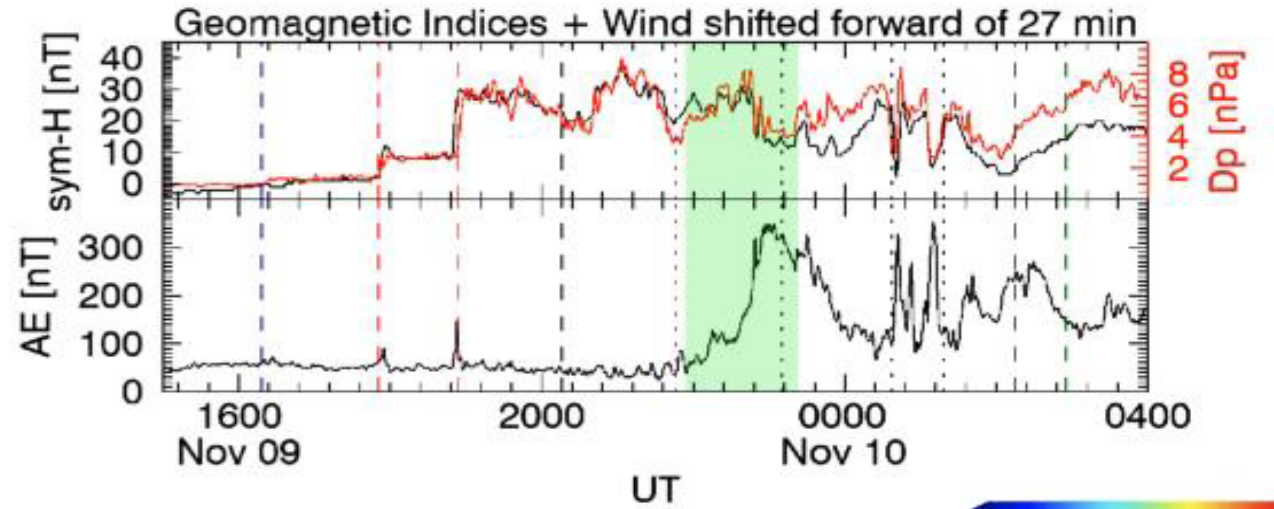
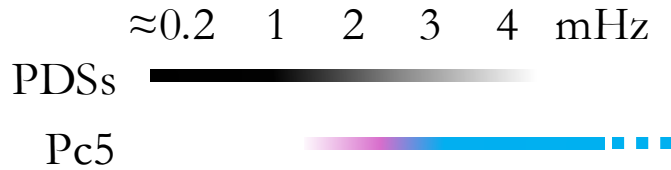


Solar wind driven fluctuations along the compressive component.

[\(Di Matteo et al., 2022\)](#)

Periodic density structures (PDSs) drive global fluctuations

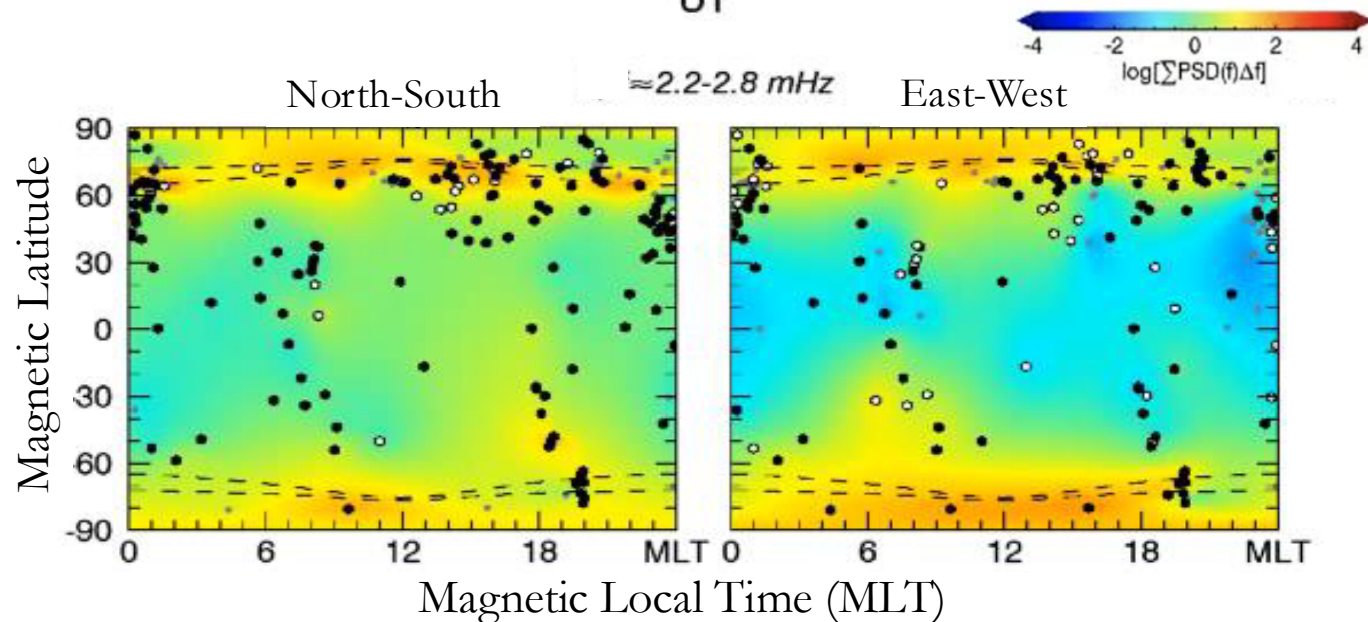
↓ $\approx 2.6\text{--}2.8$ mHz



Qualitative global map of the fluctuations power integrated **between ≈ 2.2 and ≈ 2.8 mHz**

- ground station location
- broad power enhancement
- wave at discrete frequency

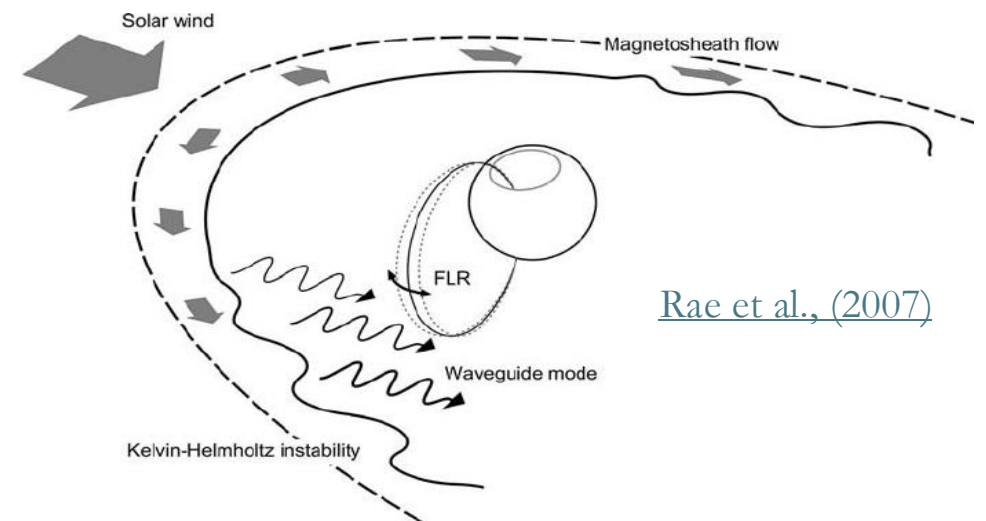
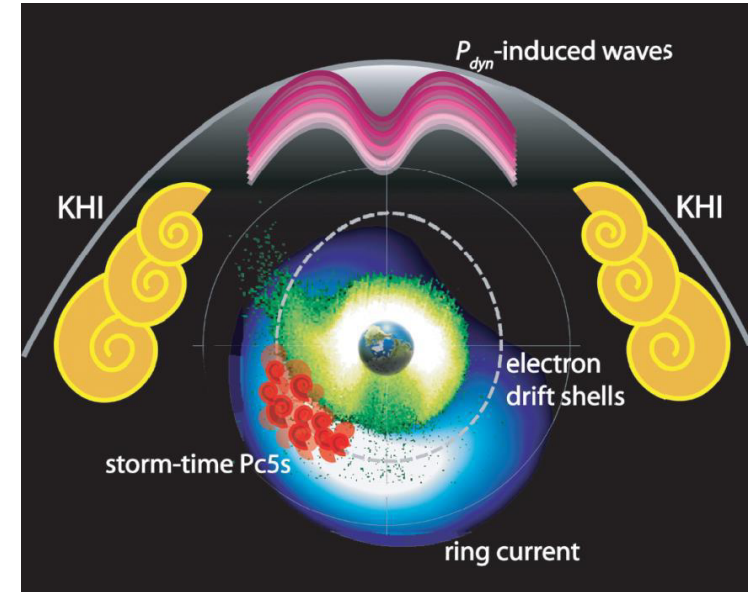
(Di Matteo et al., 2022)



Source of controversy: many different sources of waves in this frequency range?

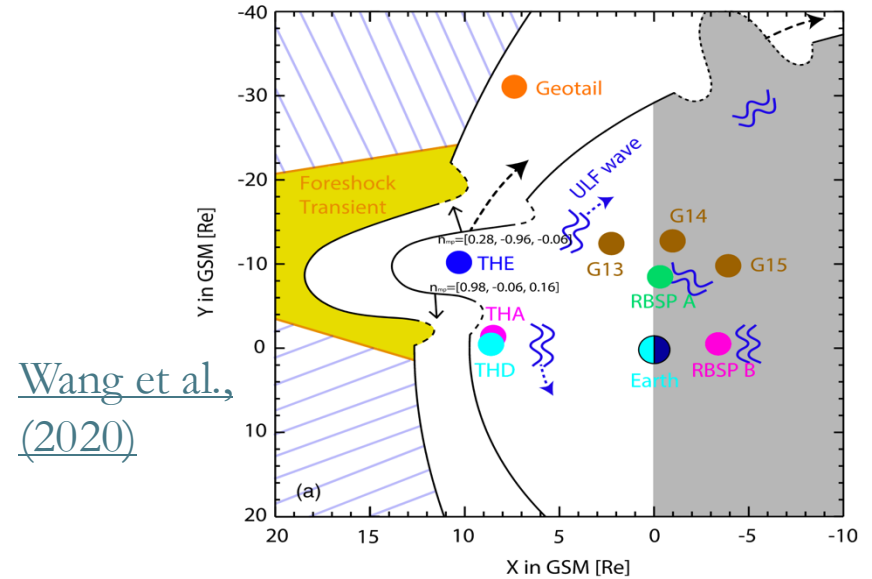
- Plasma waves with largest wavelengths and lowest frequencies in the system
 - Impact onto the magnetosphere of **interplanetary shocks or pressure impulses** ([Allan et al. 1986](#); [Southwood & Kivelson, 1990](#); [Mann et al., 1998](#));
 - **Kelvin-Helmholtz instability** at the magnetopause ([Southwood, 1974](#); [Chen & Hasegawa, 1974](#));
 - **Solar wind buffeting** ([Wright & Rickard, 1995](#));
 - **Surface waves at the magnetopause** ([Plaschke & Glassmeier, 2011](#); [Archer et al., 2019](#)) or the **plasmopause** ([He et al., 2020](#)).
 - **Ion-foreshock transients** ([Hartinger et al., 2013](#); [Wang et al., 2020](#))
 - **Directly driven by solar wind density fluctuations** ([Kepko et al, 2002](#); [Kepko et al., 2003](#); [Di Matteo et al., 2022](#))
 - **Injected energetic particles** ([Glassmeier et al., 1999](#); [James et al., 2013](#); [Yeoman et al., 2010](#))
- **Triggered fast magnetosonic waves** propagate in the magnetosphere and possibly couple with
 - **field line resonances** ([Southwood, 1974](#); [Chen & Hasegawa, 1974](#));
 - **cavity/waveguide modes** ([Kivelson & Southwood, 1985; 1986](#); [Samson et al. 1992](#); [Harrold & Samson, 1992](#)).

[Ukhorskiy et al., 2009](#)



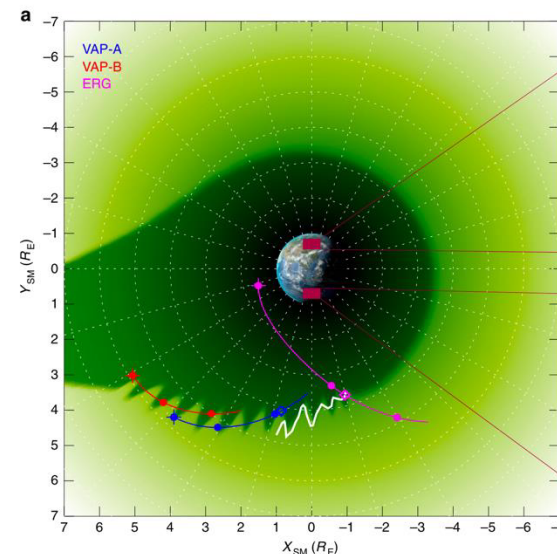
Source of controversy: many different sources of waves in this frequency range?

- Plasma waves with largest wavelengths and lowest frequencies in the system
 - Impact onto the magnetosphere of **interplanetary shocks or pressure impulses** ([Allan et al. 1986](#); [Southwood & Kivelson, 1990](#); [Mann et al., 1998](#));
 - **Kelvin-Helmholtz instability** at the magnetopause ([Southwood, 1974](#); [Chen & Hasegawa, 1974](#));
 - **Solar wind buffeting** ([Wright & Rickard, 1995](#));
 - **Surface waves at the magnetopause** ([Plaschke & Glassmeier, 2011](#); [Archer et al., 2019](#)) or the **plasmopause** ([He et al., 2020](#)).
 - **Ion-foreshock transients** ([Hartinger et al., 2013](#); [Wang et al., 2020](#))
 - **Directly driven by solar wind density fluctuations** ([Kepko et al, 2002](#); [Kepko et al., 2003](#); [Di Matteo et al., 2022](#))
 - **Injected energetic particles** ([Glassmeier et al., 1999](#); [James et al., 2013](#); [Yeoman et al., 2010](#))
- **Triggered fast magnetosonic waves** propagate in the magnetosphere and possibly couple with
 - **field line resonances** ([Southwood, 1974](#); [Chen & Hasegawa, 1974](#));
 - **cavity/waveguide modes** ([Kivelson & Southwood, 1985; 1986](#); [Samson et al. 1992](#); [Harrold & Samson, 1992](#)).

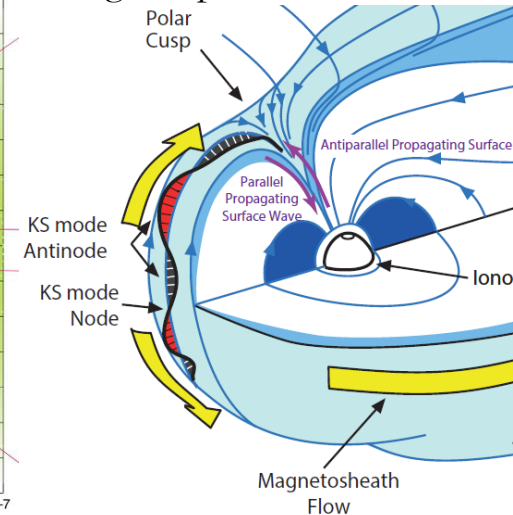


Wang et al., (2020)

He et al., 2020 Surface waves at the plasmopause



Archer & Plaschke, (2015) Surface waves at the magnetopause



ULF waves activity as consecutive driving/triggering of different modes

The emerging picture of this event is that of magnetospheric field fluctuations characterized by:

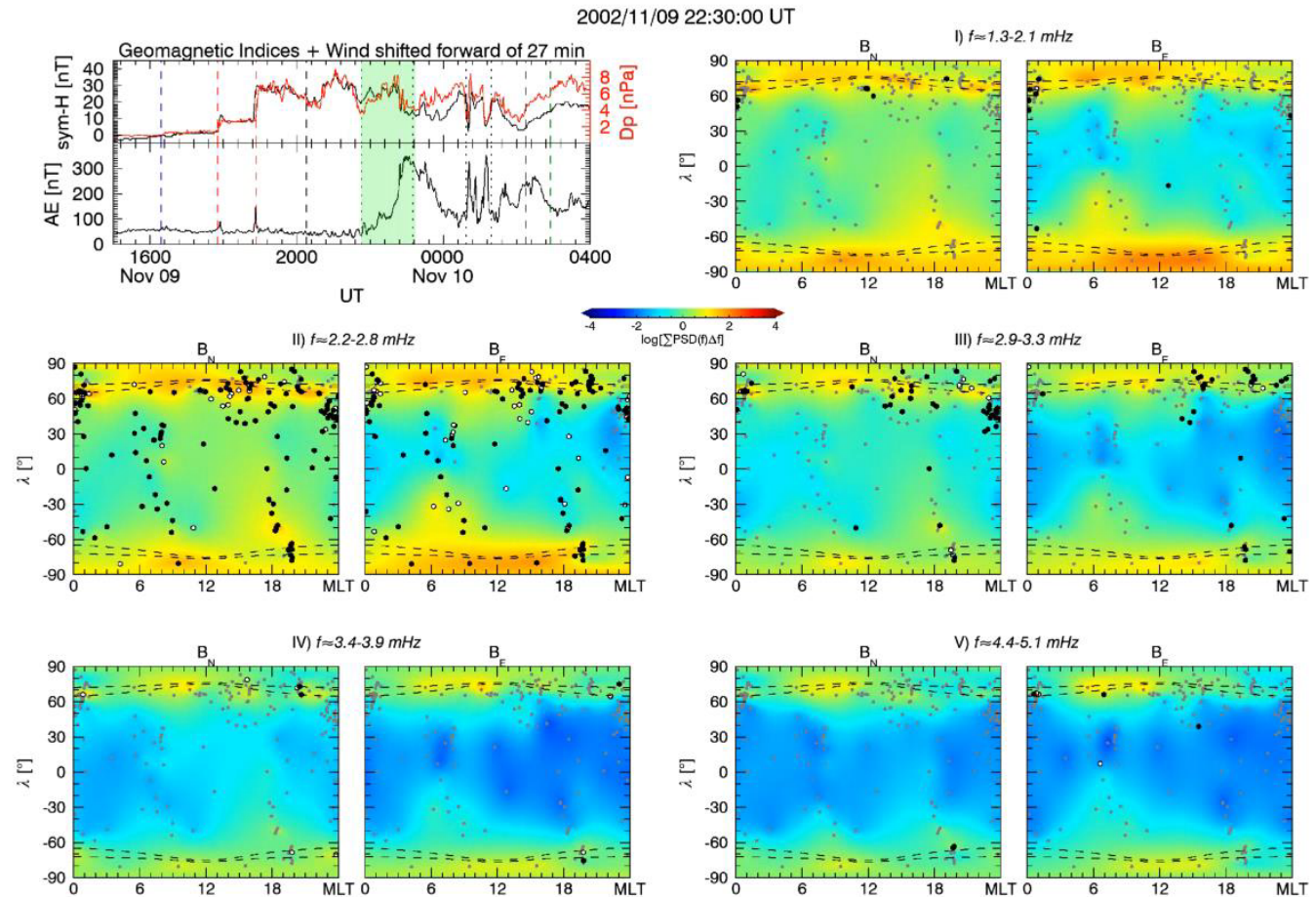
1. **Modes directly driven** by solar wind dynamic pressure below ≈ 1 mHz;
2. A **combination of directly driven oscillations and wave modes triggered** by additional mechanisms (e.g., shock and interplanetary magnetic field discontinuity impact, substorm) between ≈ 1 and ≈ 4 mHz;
3. **Internally and externally triggered** wave modes above ≈ 4 mHz.

≈ 0.2 1 2 3 4 mHz



**Directly Driven
Global**

**Triggered
more localized**



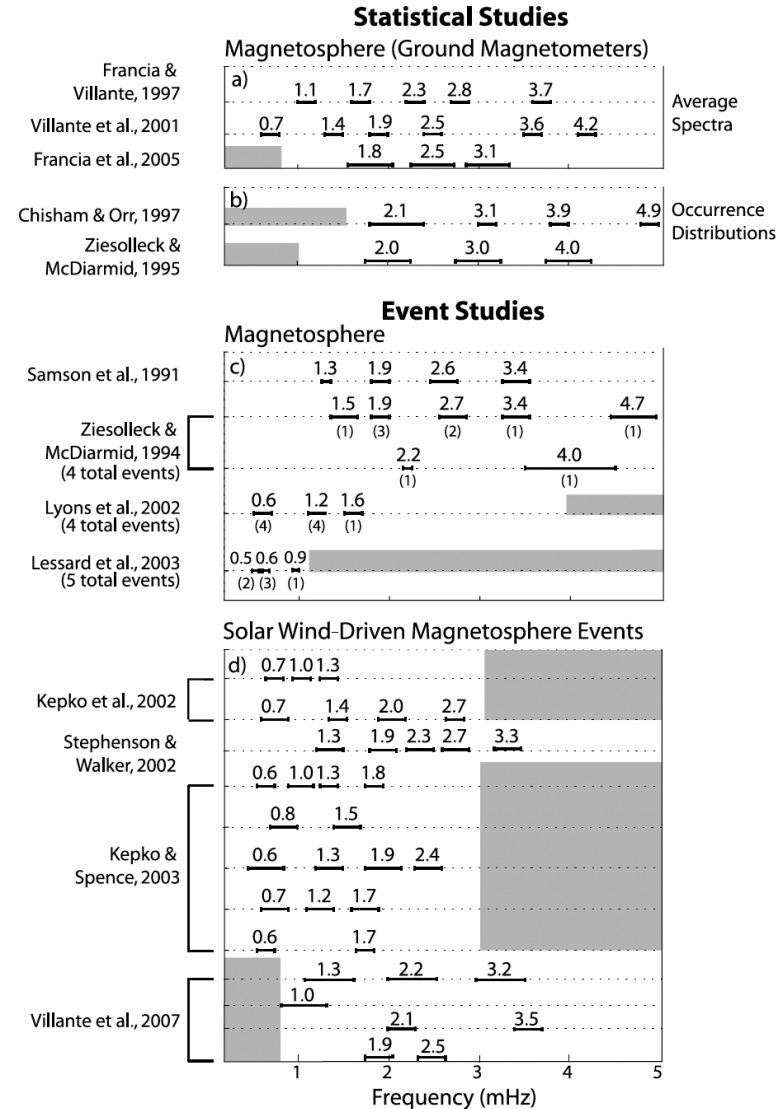
Animation available in the Supporting Information of [Di Matteo et al., \(2022\)](https://doi.org/10.1029/2021JA030144)
<https://agupubs.onlinelibrary.wiley.com/doi/full/10.1029/2021JA030144>

Magnetospheric discrete frequencies directly driven by the solar wind

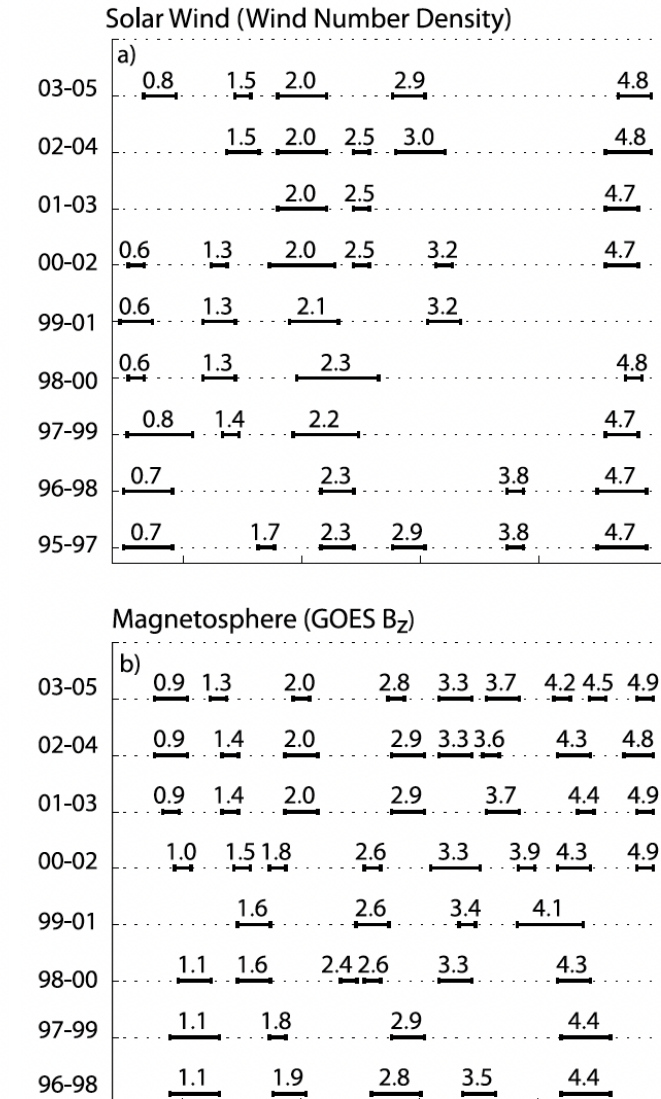
[Viall et al. \(2009\)](#) conducted a long-term statistical analysis over a solar cycle:

- certain frequencies more frequent than others
- for fluctuations of the SW number density ($f \approx 0.7, \approx 1.4, \approx 2.0,$ and ≈ 4.8 mHz)
- and in the dayside magnetospheric field ($f \approx 1.0, \approx 1.5, \approx 1.9, \approx 2.8, \approx 3.3,$ and ≈ 4.4 mHz).

Is there a relation to the ULF waves “magic frequencies”?



[Viall et al. \(2009\)](#)

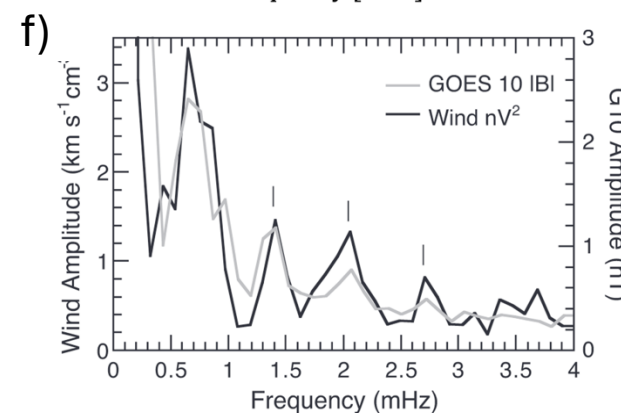
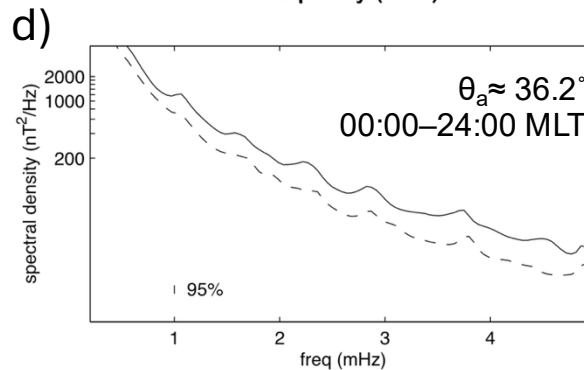
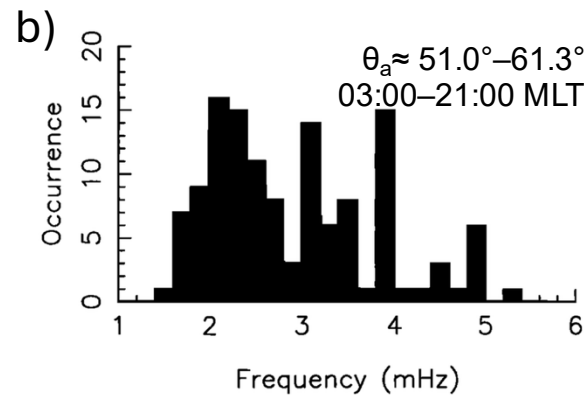
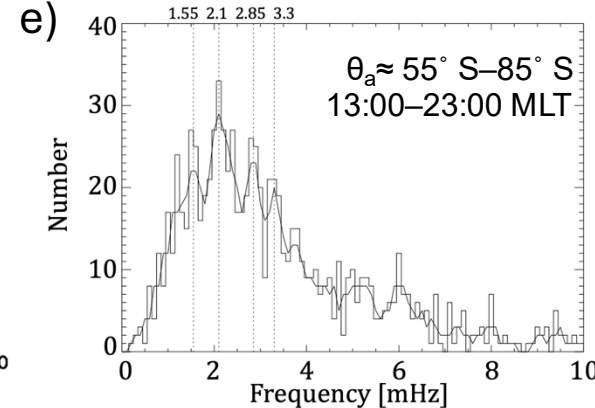
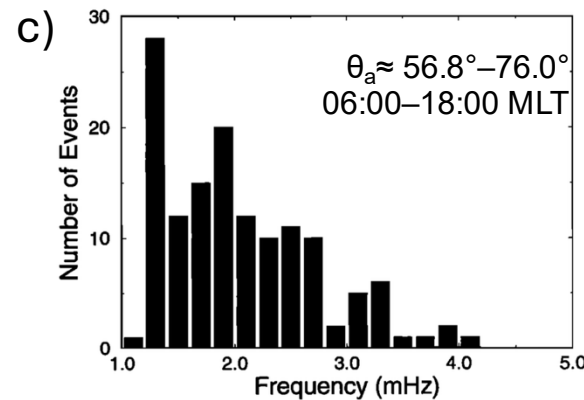
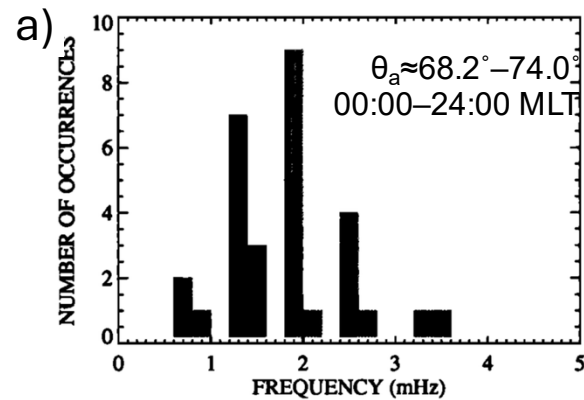


Controversy on the existence and stability of “magic” frequencies

The observation of wave packets at different discrete frequencies, approximately in the range $f \approx 1 - 5$ mHz, occurring almost simultaneously at different sites



Extensive analysis covering many years of data suggests the absence of such set of fluctuations at discrete frequencies



- a) 12 events at SuperDARN [Fenrich et al., \(1995\)](#)
- b) 129 events at SAMNET [Chisham and Orr, \(1997\)](#);
- c) 137 events at IMAGE [Mathie et al., \(1999a\)](#);
- d) average spectra at L'Aquila station over three months [Villante et al., \(2001\)](#);
- e) TIGER radars from [Norouzi-Sedeh et al. \(2015\)](#);
- f) Wind versus GOES |B| [Kepko et al. \(2002\)](#)

Controversy on the existence and stability of “magic” frequencies

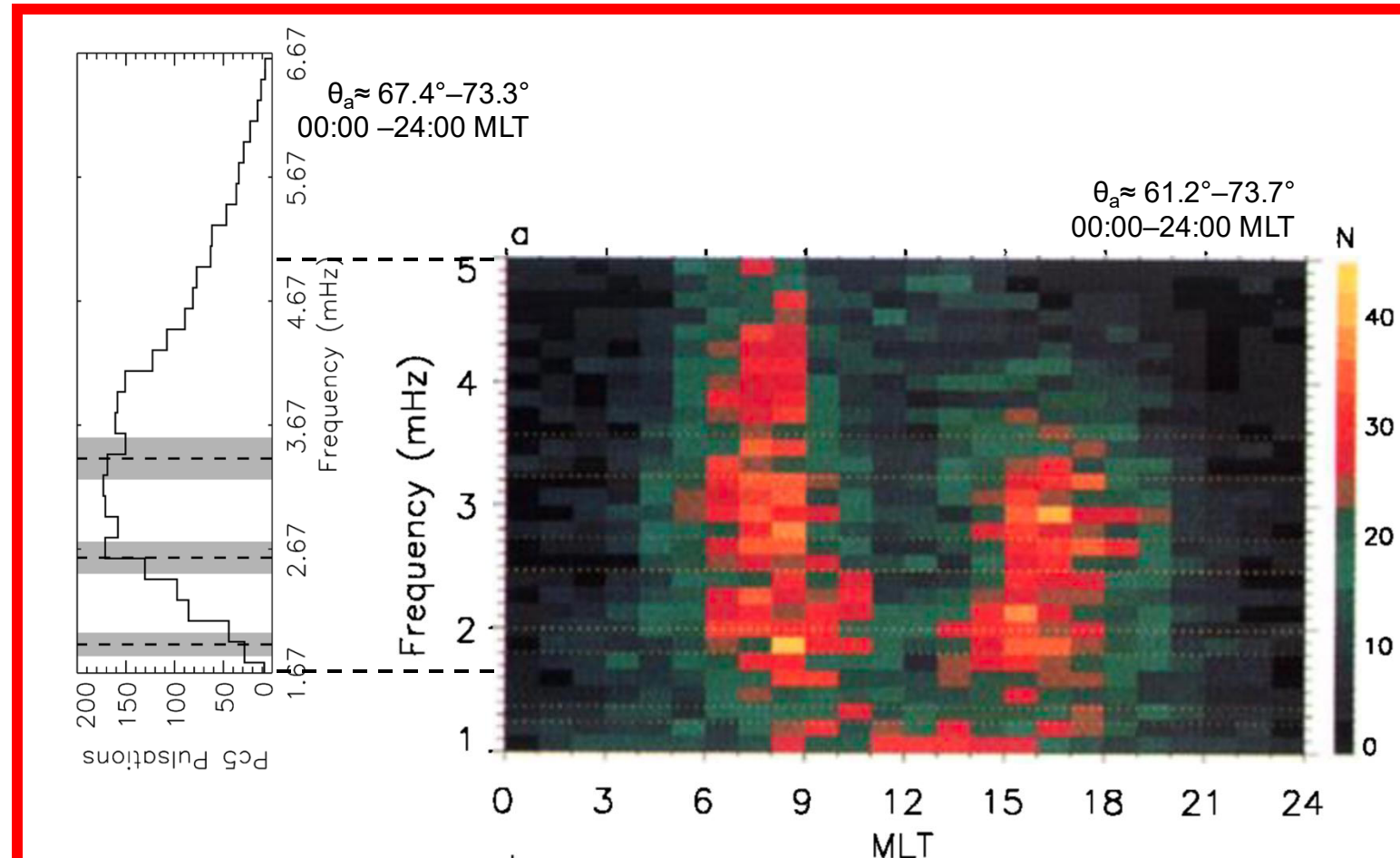
The observation of wave packets at different discrete frequencies, approximately in the range $f \approx 1 - 5$ mHz, occurring almost simultaneously at different sites



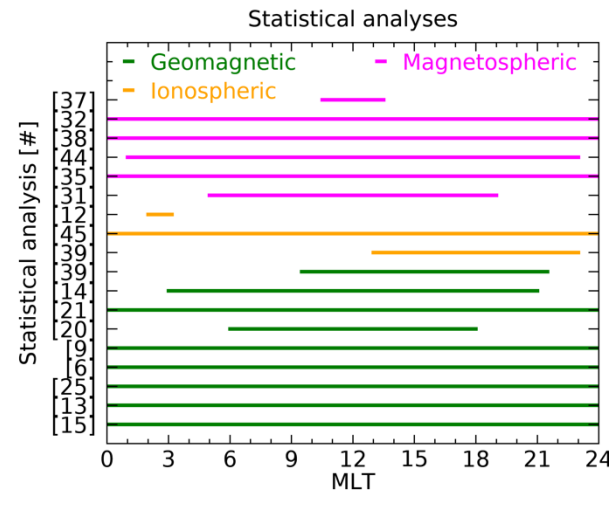
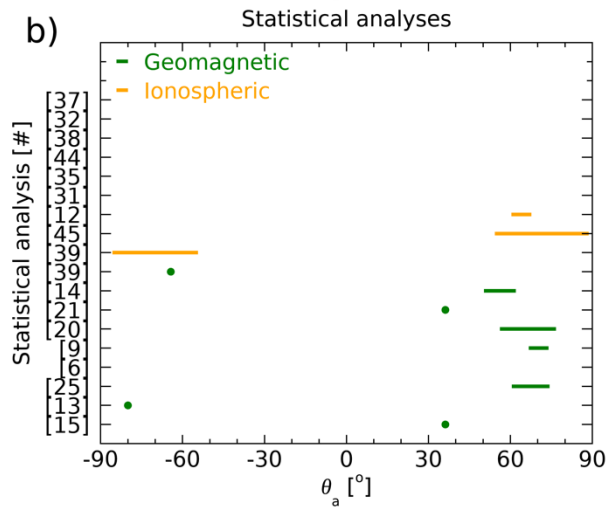
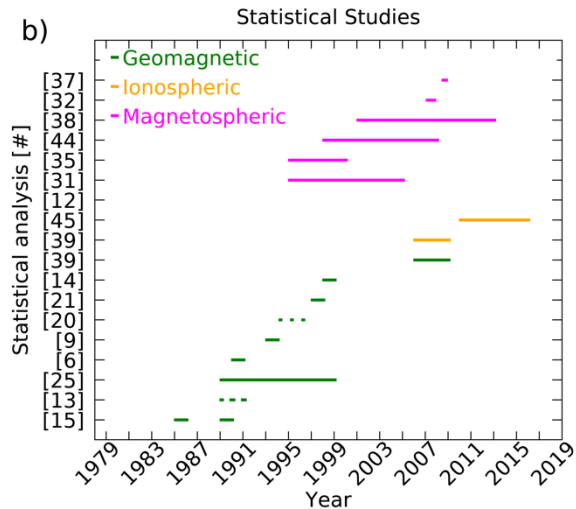
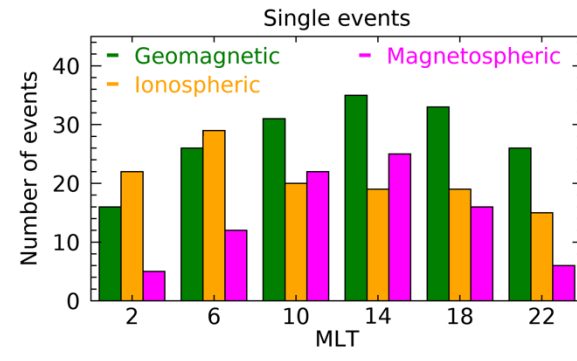
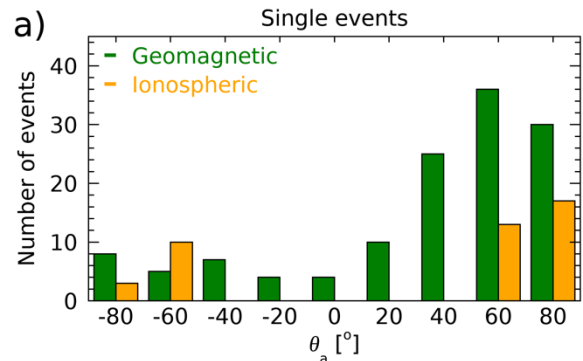
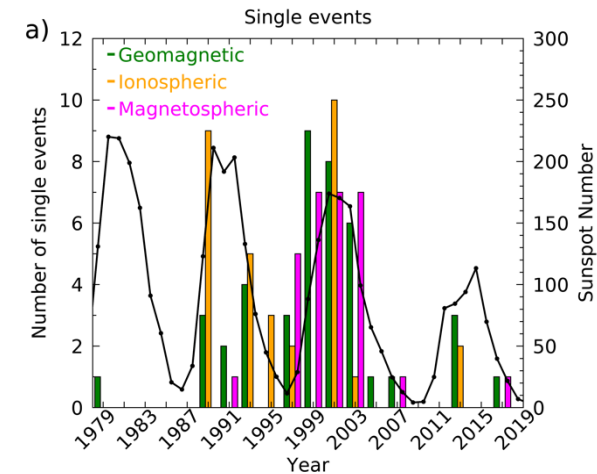
Extensive analysis covering many years of data suggests the absence of such set of fluctuations at discrete frequencies

- Left panel, the frequency distribution of events for the entire year 1993 at CANOPUS from [Baker et al. \(2003\)](#).
- Right panel, frequency/MLT distribution of events identified at six stations of the CANOPUS array from [Ziesolleck and McDiarmid \(1995\)](#); set of frequencies different from the “magic” ones are also possible.

[Di Matteo and Villante \(2025\)](#)



Comprehensive Review: Time interval, MLT, and latitudinal distribution of “magic frequencies” reports

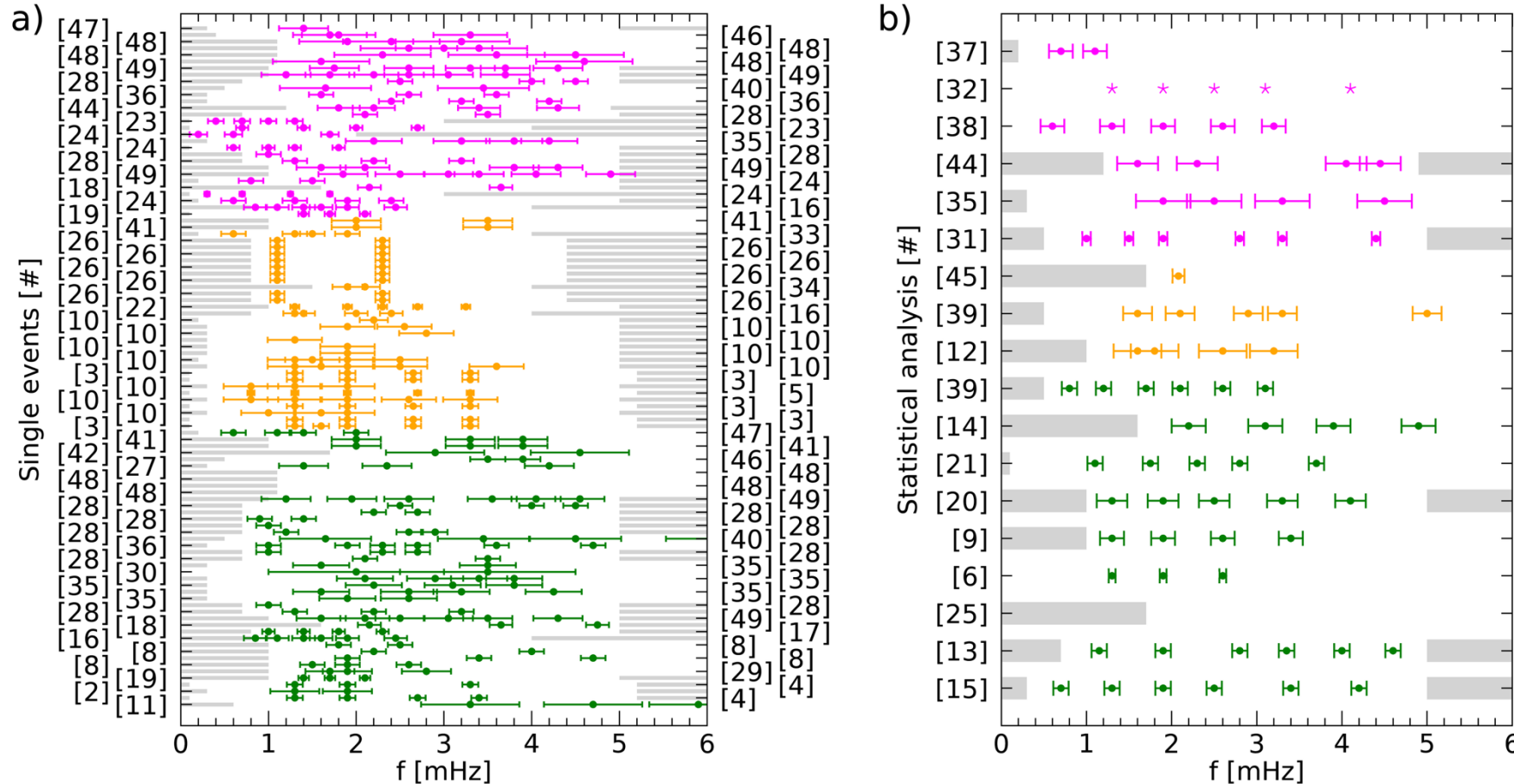


□ We collected time, location, and frequency of ULF waves occurring at a set of discrete frequencies discussed in the literature of the last 30 years.

□ The reported events concentrate during solar maximum, at high latitude and with a slight preference toward the dayside sector.

Comprehensive Review: Role of the analysis techniques

• Geomagnetic • Ionospheric • Magnetospheric

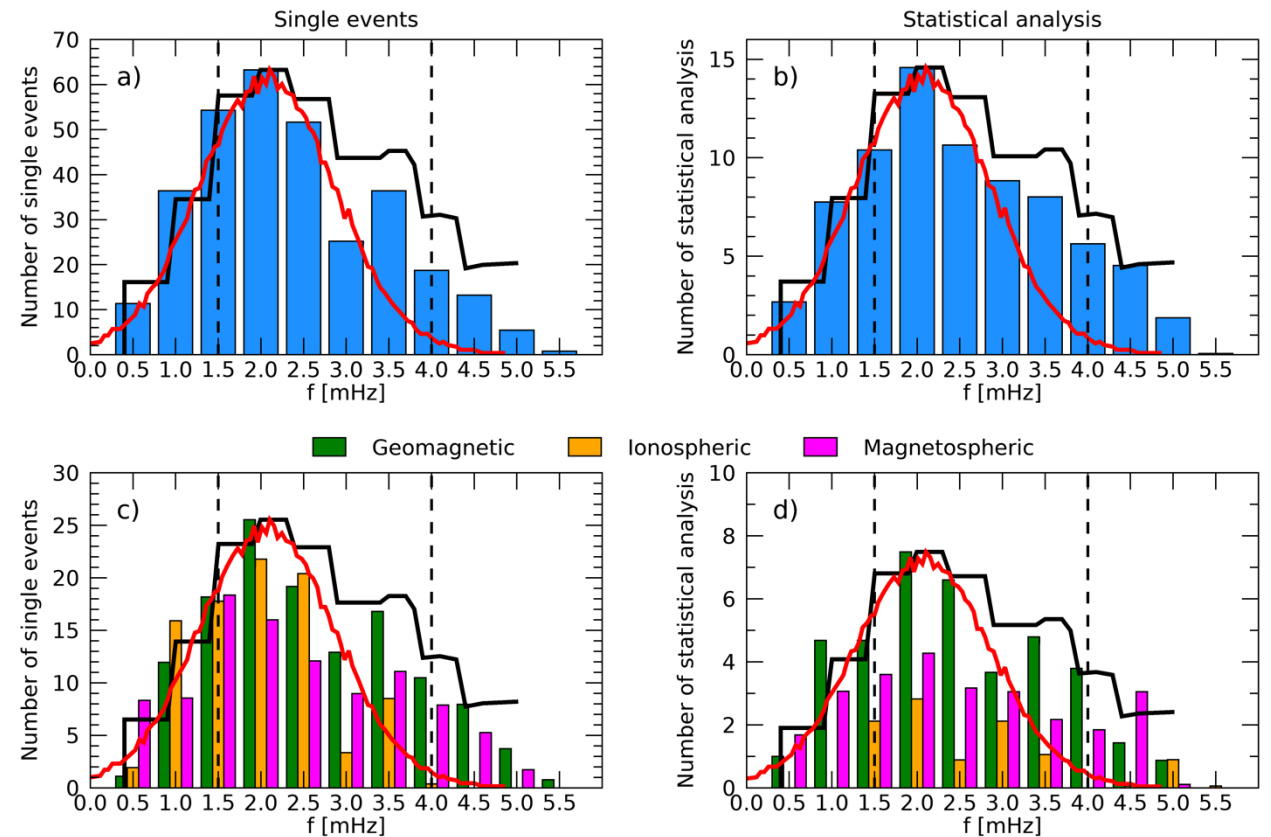


- The explored frequency ranges, limited by the grey bars, changed in each investigation. Fluctuations below ≈ 1 mHz are rarely investigated.
- The frequency resolution, indicated by the error bars depend on the methodology used to identify ULF waves.

Frequency distributions show *no absolute* set of discrete frequencies

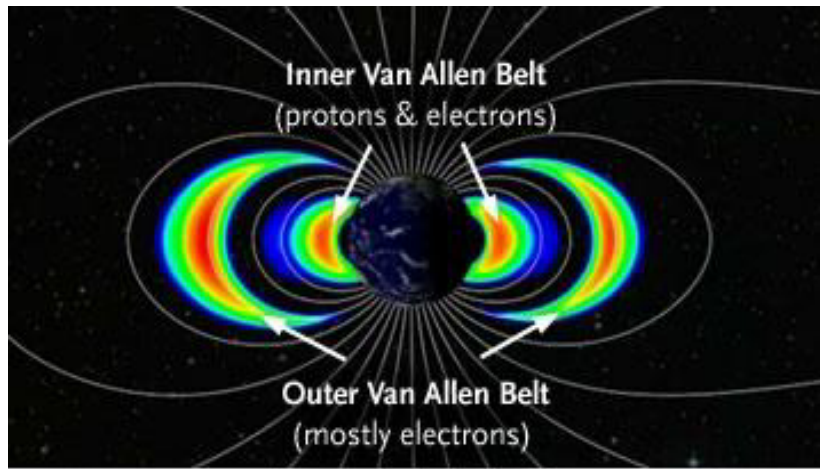
- a) Global frequency distribution combining experimental results from geomagnetic (green), ionospheric (orange), and magnetospheric (magenta) investigations which are depicted separately in panel c)
- b) The same but for statistical investigations in which we counted as a single entity the occurrence of events in each frequency band in the single analysis
- Red lines, modeled frequency distribution (not to scale) of periodic NSW structures by ([Kepko et al., 2024](#)); black lines, occurrence rate of periodicities in transverse velocity fluctuations in the solar corona ([Morton et al., 2019](#))

[Di Matteo and Villante \(2025\)](#)



PDSs driven/ULF waves provide resonant and diffusive acceleration and transport of radiation belt electrons

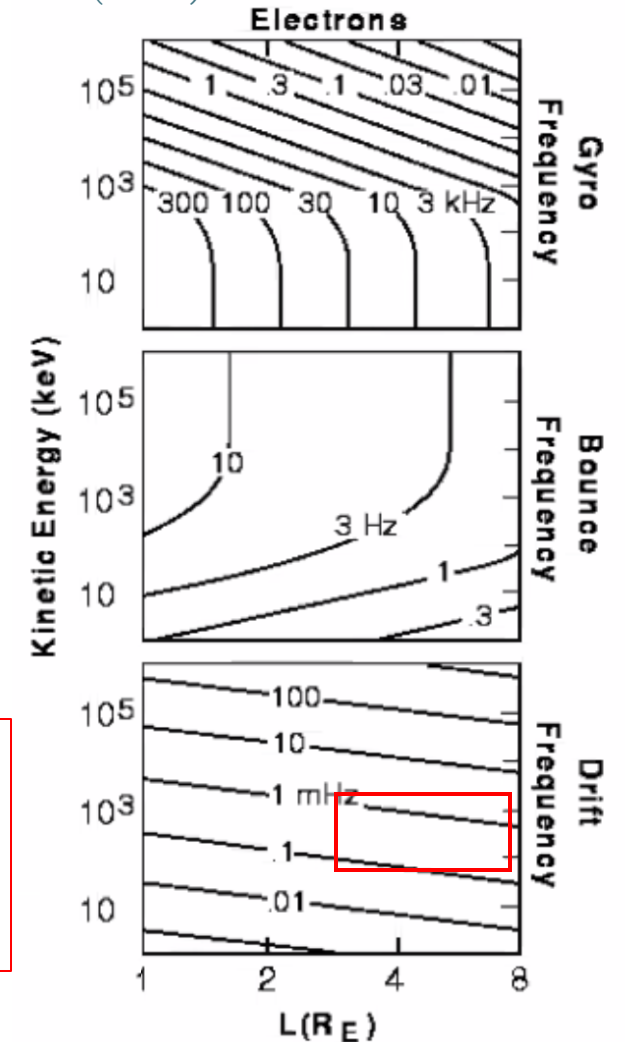
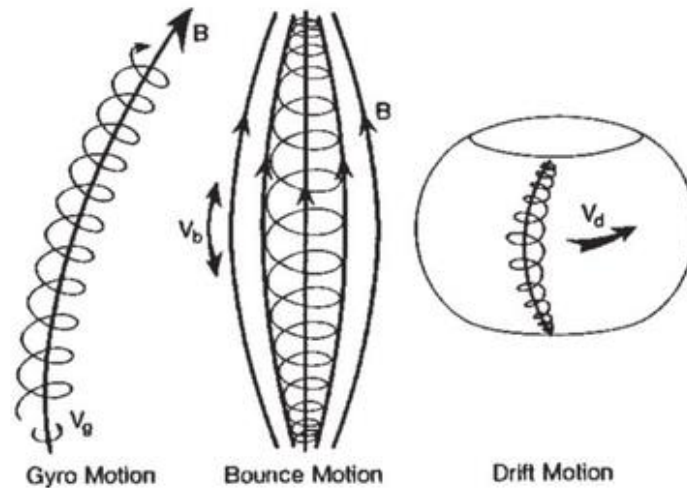
The Van Allen Radiation belts consist of energetic charged particles trapped by the Earth's magnetic field.



Credit: NASA / JHU-APL / Univ. of Colorado



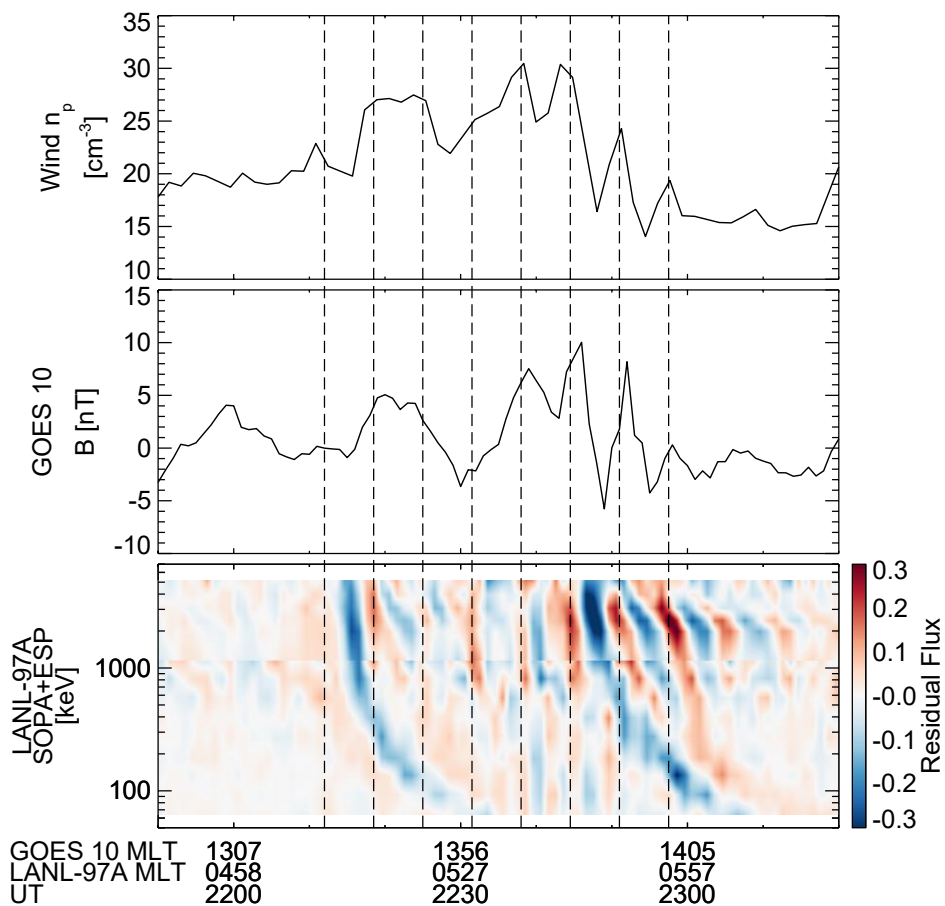
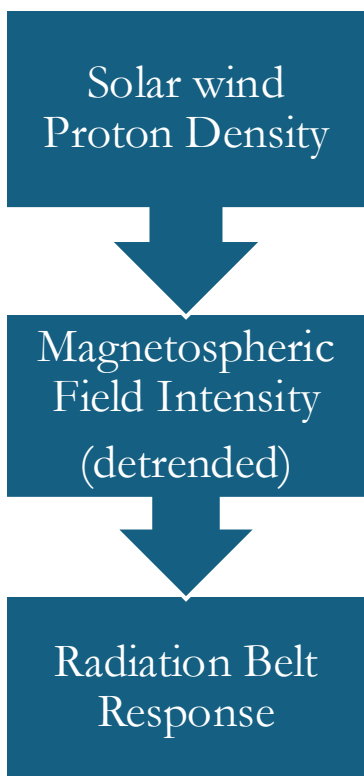
[Schulz and Lanzerotti \(1974\)](#)



Timescale relevant for the outer belt electrons drift motion.

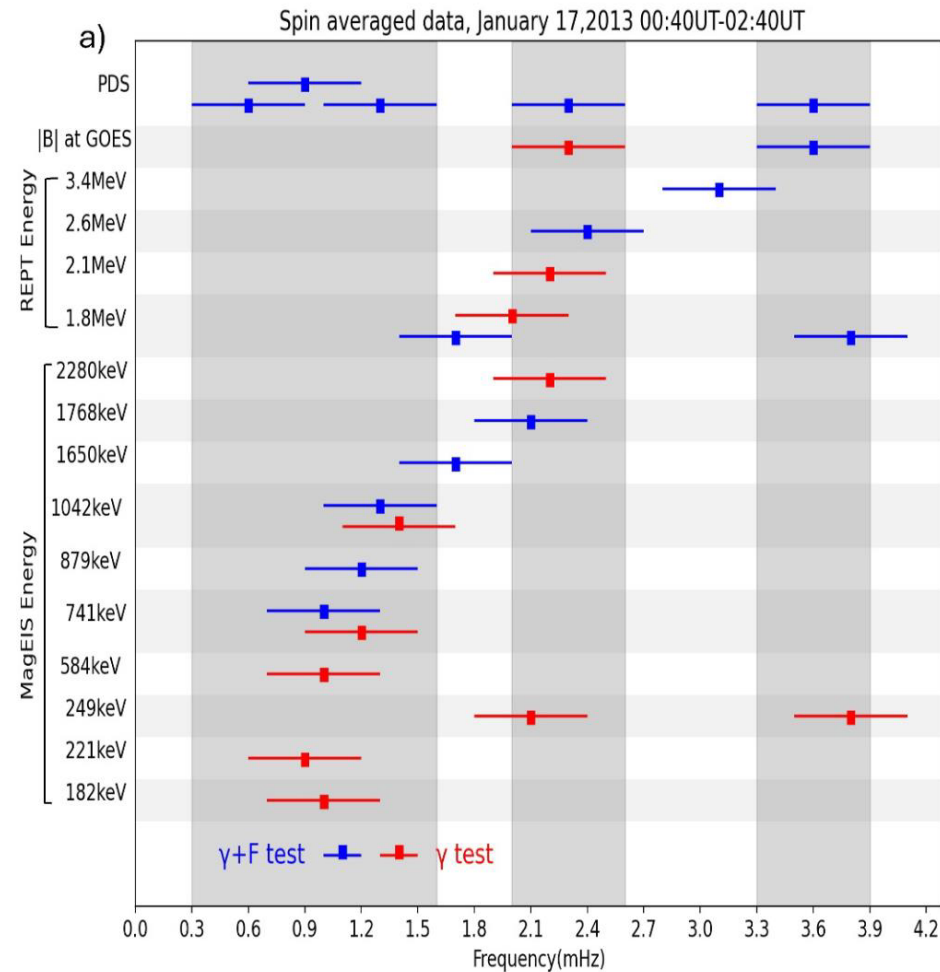
Radiation belt periodic response to solar wind driven waves

Evidence of drift resonance at ≈ 2.6 mHz for electrons at energies of ≈ 1.8 – 2.2 MeV



(Di Matteo et al., 2022)

[Kurien, Kanekal, Di Matteo et al. \(2024\)](#)



Conclusions

- Understanding the properties of solar wind mesoscale structures will shed new light:
 - on their formation mechanism, imposing constraints on solar wind models
 - on their impact on Earth... and other planetary systems?
- The next era of multi-spacecraft fleets provide a great opportunity to move beyond general assumptions, heritage of an era based on isolated single spacecraft missions.
- We now have:
 - More data/multipoint observations
 - Computational capabilities to analyze them
 - Sophisticated model for comparison

Let's walk that "yellow brick road"
to reach across scales
and systems,
together!